Available online at www.sciencedirect.com
ScienceDirect
Journal of Computational Physics 224 (2007) 182–207
JOURNAL OF COMPUTATIONAL PHYSICS
www.elsevier.com/locate/jcp

Design principles for bounded higher-order convection schemes – a unified approach

N.P. Waterson [a,*], H. Deconinck [b]

[a] Department of Aeronautics, Imperial College London, Prince Consort Road, London SW7 2AZ, UK
[b] von Karman Institute for Fluid Dynamics, Waterloosesteenweg 72, B-1640 Sint-Genesius-Rode, Belgium

Received 12 October 2006; received in revised form 18 January 2007; accepted 25 January 2007
Available online 2 February 2007

Abstract

The design of bounded, higher-order convection schemes is considered with a view to selecting those discretizations giving good resolution of sharp gradients, while at the same time providing competitive accuracy and convergence behaviour when applied to smooth, recirculating flows. The present work contains a detailed classification and analysis and extensive tables of most non-linear scalar convection schemes so far proposed within the cell-centred, finite-volume framework. The analysis includes a review and comparison of the two most frequently-used non-linear approaches, flux limiters (FL) and normalized variables (NV), and the three major boundedness criteria typically employed: *total-variation diminishing* (TVD), *positivity* and the *convection-boundedness criterion* (CBC). All NV schemes considered are converted to FL form to allow direct comparison and classification of a wide range of schemes. Several specific design principles for *positive non-linear schemes* are considered and it is shown how these can be applied to understand the relative performance of different approaches. Finally the performance of many existing schemes is compared and ranked on the basis of two scalar convection test cases, one smooth and one discontinuous, which demonstrates the wide variation in both accuracy and convergence behaviour of the various schemes and the benefits of the design principles considered.

Keywords: Convection; Discretization; Non-linear; Bounded; Higher-order; TVD; Flux limiters; Normalized variables

1. Introduction

The discretization of the terms representing convective transport remains one of the most challenging aspects in the numerical simulation of fluid-flow phenomena. In the context of the *cell-centred*, *finite-volume* discretizations considered here, the introduction of second-order upwind-biased schemes from the 1960s onwards marked a major step forward, allowing more accurate solutions of convection-dominated flows at higher Reynolds numbers.

* Corresponding author. Tel.: +44 (0)20 7594 1975; fax: +44 (0)20 7584 8120.
E-mail address: n.waterson@imperial.ac.uk (N.P. Waterson).

0021-9991/$ - see front matter
doi:10.1016/j.jcp.2007.01.021

Such *linear* convection schemes, although more stable than pure central differencing and more accurate than first-order upwinding (FOU), still remain vulnerable to unphysical oscillations under some circumstances, in particular in the presence of sharp gradients. This limitation is predicted by Godunov's famous theorem [40] stating that no linear convection scheme of second-order accuracy or higher can be monotonic. The answer has been the use of *non-linear* discretizations, which adjust themselves according to the local solution so as to maintain bounded behaviour.

Though it is now well-known that the use of non-linear convection schemes can lead to solutions combining boundedness and accuracy, it is clear from published literature and industrial practice that the wide variation in the performance of such schemes, and the principles for their appropriate selection, are much less well understood. In [59] the present authors undertook a study to classify and analyze non-linear schemes and to design new ones suitable for the wide range of flows typical of industrial applications. Particular attention was paid to those discretizations giving good resolution of sharp gradients, while at the same time providing competitive accuracy and convergence behaviour when applied to smooth, recirculating flows. The present work expands and updates significantly the earlier study including a more detailed classification and analysis and extensive tables of most non-linear scalar convection schemes so far proposed, within the cell-centred, finite-volume framework.

The analysis includes a review and comparison of the two most frequently-used non-linear approaches, that is flux limiters (FL) and normalized variables (NV), and the three major boundedness criteria typically employed: *total-variation diminishing* (TVD), *positivity* and *the convection-boundedness criterion (CBC)*. All NV schemes considered are converted to FL form to allow direct comparison and classification of a wide range of schemes. Several specific design principles for *positive, non-linear schemes* are considered and it is shown how these can be applied to understand the relative performance of different approaches. Finally the performance of many existing schemes is compared and ranked on the basis of two scalar convection test cases, one smooth and one discontinuous, which demonstrates the wide variation in both accuracy and convergence behaviour of the various schemes and the benefits of the design principles considered.

Only steady-state, cell-centred, finite-volume solutions of convective conservation laws are considered, for which a model problem is the linear, scalar convection equation:

$$\mathbf{u}(x,y,z)\cdot\nabla\phi = 0, \tag{1}$$

where ϕ is a scalar variable being convected by a velocity field $\mathbf{u}(x,y,z)$.

The finite-volume discretization for a whole cell may be summarized as:

$$\sum_{nb} a_{nb}(\phi_{nb}-\phi_P) = 0, \tag{2}$$

where ϕ_P is the cell-averaged value of the variable stored at the cell centre, ϕ_{nb} the values at the cell neighbours and a_{nb} the discretization coefficients. The particular procedure by which this system of equations may be resolved will not be considered here. All of the discretizations considered will be of a cell-centred, finite-volume variety and all will be "dimensionally split", that is 2D and 3D implementations will consist of one-dimensional schemes applied separately along each of the grid directions.

The key problem in defining cell-centred finite-volume discretizations is the interpolation of *cell-face values* of the convected variable from the *cell-averaged values*, stored at the cell centres. All of the schemes considered here calculate face values using at most three cell-centre values (giving a five-node stencil for a whole cell) and all may be described using the upwind-biased stencil shown in Fig. 1. It should be noted that all of the convective discretizations described here may be applied to time-varying problems when combined with an appropriate temporal discretization and time-step restriction.

2. Linear schemes

Many well-known linear, higher-order schemes may be expressed conveniently as members of the class of so-called κ-schemes, developed originally as part of van Leer's variable-extrapolation, MUSCL approach [52,53]. The κ-scheme formulation will be reviewed here both because it forms a helpful framework within

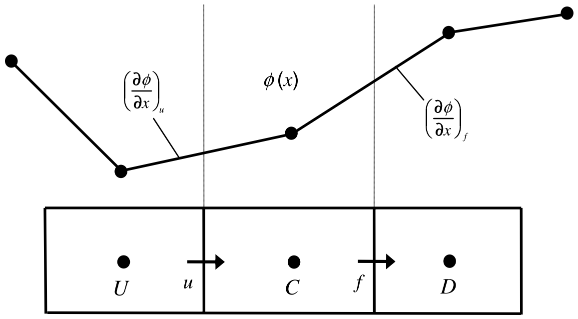

Fig. 1. Sketch of upwind-biased stencil and notation.

which to analyze linear schemes and because it provides a platform for the construction and interpretation of non-linear schemes.

2.1. κ-scheme formulation

The cell-face value of the convected variable, predicted by the κ-schemes, may be written, using the notation outlined above, either as the first-order upwind (FOU) scheme enhanced by an additional "*anti-diffusive*" term:

$$\phi_f = \phi_C + \left\{\frac{1+\kappa}{4}(\phi_D - \phi_C) + \frac{1-\kappa}{4}(\phi_C - \phi_U)\right\} \tag{3}$$

or as the central-difference scheme with the addition of a stabilizing, upwind-biased "*artificial-dissipation*" term:

$$\phi_f = \frac{1}{2}(\phi_C + \phi_D) - \frac{1-\kappa}{4}(\phi_D - 2\phi_C + \phi_U). \tag{4}$$

Both of these expressions assume a uniform grid spacing however the generalization to non-uniform grid spacing is quite straightforward:

$$\phi_f = \phi_C + \frac{\Delta x_C}{2}\left\{\frac{(1+\kappa)}{2}\left(\frac{\partial \phi}{\partial x}\right)_f + \frac{(1-\kappa)}{2}\left(\frac{\partial \phi}{\partial x}\right)_u\right\}, \tag{5}$$

where $\Delta x_C = x_f - x_u$ and:

$$\left(\frac{\partial \phi}{\partial x}\right)_f = \frac{\phi_D - \phi_C}{x_D - x_C}, \quad \left(\frac{\partial \phi}{\partial x}\right)_u = \frac{\phi_C - \phi_U}{x_C - x_U}. \tag{6}$$

It can be seen clearly from the upwind formulation in (5) that the higher-order correction employs a linear weighted average of two local gradients of the convected variable: one across the cell face in question and the second immediately upwind, see Fig. 1. The weighting is controlled by the variable κ, with a value of $\kappa = 1$ eliminating the upwind gradient and a value of $\kappa = -1$ eliminating the centred gradient. Similarly it can be seen from the artificial-dissipation form (4) that $\kappa = 1$ eliminates the artificial viscosity term while for values of $\kappa < 1$ its magnitude increases as κ decreases. The average of the gradients is convex for values of κ in the range $[-1, 1]$.

Several well-known higher-order convection schemes are represented by different values of κ, given here in the order of increasing upwind bias (and summarized in Table A1):

- $\boldsymbol{\kappa = 1}$: *central difference* (*CDS*) – the only κ-scheme with no upwind bias, face value calculated by linear interpolation from the two adjoining nodal values.

- $\boldsymbol{\kappa} = \frac{1}{2}$: *quadratic-upwind interpolation* (*QUICK*) [25] – face value calculated by quadratic interpolation through three nodes, two upwind and one downwind. This gives a third-order approximation for the face value though only a second-order approximation for the whole cell.
- $\boldsymbol{\kappa} = \frac{1}{3}$: *cubic-upwind interpolation* (*CUI*) [1] – unique third-order κ-scheme. Proposed by Agarwal [1] in a finite-difference context where it is equivalent to fitting a cubic polynomial through a four-point upwind-biased stencil. The term "CUI" is not strictly consistent with "LUI" or "QUICK" but is a convenient shorthand which will be followed here.
- $\boldsymbol{\kappa} = \mathbf{0}$: *Fromm's scheme* [13] – specially designed to minimize dispersion error and uniquely symmetric with equal weighting given to the centred and upwind gradients.
- $\boldsymbol{\kappa} = -\mathbf{1}$: *linear-upwind interpolation* (*LUI*) [4,36,57] – the only fully upwind κ-scheme, with the face value calculated by linear extrapolation from the two upwind nodal values. Sometimes referred to as "second-order upwind" (SOU).

All of these schemes require at most a five point stencil in one dimension and all are linear when applied to the linear advection equation. In addition it may be shown that none of the schemes are bounded, *i.e.* all allow unphysical spatial oscillations in the solution under some circumstances, as predicted by Godunov's theorem [40] and discussed further below.

2.2. Accuracy and the modified differential equation

It is of interest here to examine the accuracy of these linear schemes using the modified or equivalent differential equation which gives some indication of the actual equation being solved and to what extent this differs from the original continuous equation. The modified differential equation for the steady, linear advection equation, in one dimension, discretized using the κ-schemes may be written as:

$$u\phi_x = -\frac{1}{12}(3\kappa - 1)u\Delta x^2\phi_{xxx} + \frac{1}{8}(\kappa - 1)u\Delta x^3\phi_{xxxx} + \cdots. \tag{7}$$

In this equation terms appearing on the left-hand side represent the original continuous equation while those on the right-hand side represent the leading terms of the truncation error introduced by the discretization. Of the two leading terms in the truncation error, the first is dispersive in nature and the second dissipative, the implications of which are discussed for example in [28]. In the unsteady case additional terms would appear on the right-hand side depending upon the specific time discretization considered.

The modified equation reveals immediately that all of the κ-schemes possess at least second-order truncation errors. Only for the $\kappa = \frac{1}{3}$ (CUI) scheme is the leading dispersive term in the truncation error eliminated entirely, leading to third-order accuracy. It should be noted that from the point of view of practical application the size alone of the truncation error may not be the only factor of importance – its nature can also have serious implications for convergence behaviour, as discussed further below. Table 1 summarizes the relative slope weighting factors for various κ-schemes along with the coefficients of the two leading terms on the right-hand side of the modified equation.

It is also instructive to consider the modified equation for the case of a cell having different κ-schemes, κ_u and κ_f, applied respectively to the cell faces u and f (see Fig. 1):

Table 1
Gradient weighting factors and modified-equation coefficients for various κ-schemes

κ-scheme	Centred weighting	Upwind weighting	Δx^2 coefficient	Δx^3 coefficient
1	1	0	$-\frac{1}{6}$	0
$\frac{1}{2}$	$\frac{3}{4}$	$\frac{1}{4}$	$-\frac{1}{24}$	$-\frac{1}{16}$
$\frac{1}{3}$	$\frac{2}{3}$	$\frac{1}{3}$	0	$-\frac{1}{12}$
0	$\frac{1}{2}$	$\frac{1}{2}$	$\frac{1}{12}$	$-\frac{1}{8}$
-1	0	1	$\frac{1}{3}$	$-\frac{1}{4}$

$$u\phi_x = \frac{1}{2}(\kappa_u - \kappa_f)u\Delta x\phi_{xx} - \frac{1}{12}(3\kappa_u - 1)u\Delta x^2\phi_{xxx} + \frac{1}{8}\left(\frac{7\kappa_u}{6} - \frac{\kappa_f}{6} - 1\right)u\Delta x^3\phi_{xxxx} + \dots \quad (8)$$

It can be seen that this introduces a leading first-order term whose coefficient depends on the difference in the κ values and falls in the range $[-1, 1]$, with the extreme values representing combinations of $\kappa = 1$ and -1. The magnitude of this coefficient can therefore be even larger than that for the first-order upwind scheme, which is $\frac{1}{2}$. Many of the non-linear schemes considered below use combinations of κ-schemes, even for smooth solutions, and hence will tend to introduce this first-order term to a varying extent.

It should be noted that the above analysis only applies strictly to the one-dimensional steady case on uniform grids, and then only to smooth solutions, however it is very instructive in giving a qualitative understanding of the relative behaviour of different schemes. While the κ-schemes will not maintain strict second-order accuracy on non-uniform meshes they are still *linearity preserving* (*i.e.* respecting a linear solution) if implemented using the form (5).

2.3. Comparative performance of linear schemes

In [58] the performance of the above κ-schemes, along with a number of non-linear schemes, all implemented in deferred-correction form, was examined for several high-Reynolds-number laminar incompressible flows with significant recirculation and in [59] a similar assessment was carried out for two scalar advection cases. The results from the scalar advection tests in [59] are summarized in Table B1 and discussed in more detail in Section 7. It was found for the smooth cases that in practice the CUI, Fromm's and QUICK schemes gave very similar results which were close to the reference solutions already at medium grid levels, while both CDS and LUI were noticeably less accurate. In terms of convergence behaviour, Fromm's scheme showed significant advantages over the other higher-order schemes considered. It required less under-relaxation and achieved the specified convergence criterion with approximately 25% less CPU time than the CUI and QUICK schemes, which were themselves somewhat faster than LUI and CDS. This favourable convergence behaviour is also generally reflected in the various flux-limited forms of Fromm's scheme, considered below.

3. Non-linear schemes – flux-limiter approach

Linear schemes, in particular members of the κ-family, which employ upwind-biased higher-order discretizations, have been used with some success in the discretization of convection terms for a number of years. Such linear schemes, though more stable than pure central differencing, still however remain vulnerable to unphysical spatial oscillations (wiggles) under some circumstances.

This limitation is predicted by Godunov's theorem [40] which states that no linear convection scheme with greater than first-order truncation error can be monotonic. The answer to this problem has been the use of *non-linear* discretizations, that is schemes which adjust themselves in some way according the local solution values so as to maintain bounded behaviour. One of the most effective approaches to constructing non-linear schemes has proved to be use of "flux limiters" – simple functions which define the convection scheme based on a ratio of local gradients in the solution field [46,47].

3.1. Flux-limiter formulation

The basic flux-limiter formulation used here follows that of Roe in [39] and differs from that of Sweby [46,47] and Roe in [38,40] in that the spatial terms are divorced entirely from the time discretization used (if any). This is more appropriate for pressure-based solutions of viscous flows and may be extended easily to time-varying cases using standard time-step treatments.

As shown by Roe [39], non-linear, flux-limited convection schemes can be developed quite naturally as a generalization of the κ-scheme formula in Eq. (5), by expressing the higher-order correction as a general weighted average of the centred and upwind gradients in the solution:

$$\phi_f = \phi_C + \frac{\Delta x_C}{2} B\left[\left(\frac{\partial \phi}{\partial x}\right)_f, \left(\frac{\partial \phi}{\partial x}\right)_u\right]. \tag{9}$$

The non-linear averaging function $B(p, q)$ is designed to give higher-order accuracy where possible while ensuring that some prescribed boundedness criterion is fulfilled. $B(p, q)$ must be homogeneous and thus (9) may be rewritten more conveniently as:

$$\phi_f = \phi_C + \frac{\Delta x_C}{2} \Psi(r) \left(\frac{\partial \phi}{\partial x}\right)_u, \tag{10}$$

where $\Psi(r) = B(r, 1)$ is termed a *limiter function* and the gradient ratio r is defined as:

$$r = \left(\frac{\partial \phi}{\partial x}\right)_f \Big/ \left(\frac{\partial \phi}{\partial x}\right)_u, \tag{11}$$

which simplifies in the case of a uniform mesh to:

$$r = \frac{\phi_D - \phi_C}{\phi_C - \phi_U}. \tag{12}$$

It should be noted that some authors define r using the reciprocal of the above expressions which changes the form of non-symmetric limiters but leaves symmetric ones unaltered.

Certain *linear* limiter functions recover familiar *linear* schemes, for example $\Psi(r) = 0$ gives first-order upwind, and the limiter corresponding to the κ-schemes is:

$$\Psi(r) = \frac{(1+\kappa)}{2} r + \frac{(1-\kappa)}{2}. \tag{13}$$

Hence $\Psi(r) = r$ represents the central-difference scheme, $\Psi(r) = 1$ linear-upwind interpolation and all other κ-schemes fall in the region enclosed by these two lines. These linear schemes therefore appear as straight lines in the Sweby *flux-limiter diagram* [46,47], which takes the form of a plot of $\Psi(r)$ against r, as shown in Fig. 2. Some general properties of flux-limiter functions, both desirable and undesirable, are discussed in Section 5.

Various significant regions can be identified in the FL diagram, based on the value of the gradient ratio, r. The $r = 0$ axis separates extrema ($r < 0$) from monotonic solutions ($r \geqslant 0$) and within the monotonic region $r \approx 1$ represents smooth, monotonic solutions ($r = 1$ implies linear variation). Regions of significant monotonic solution curvature, associated with discontinuities, can be identified by $r \geqslant 0$ and $r \ll 1$ (negative curvature) or $r \gg 1$ (positive curvature).

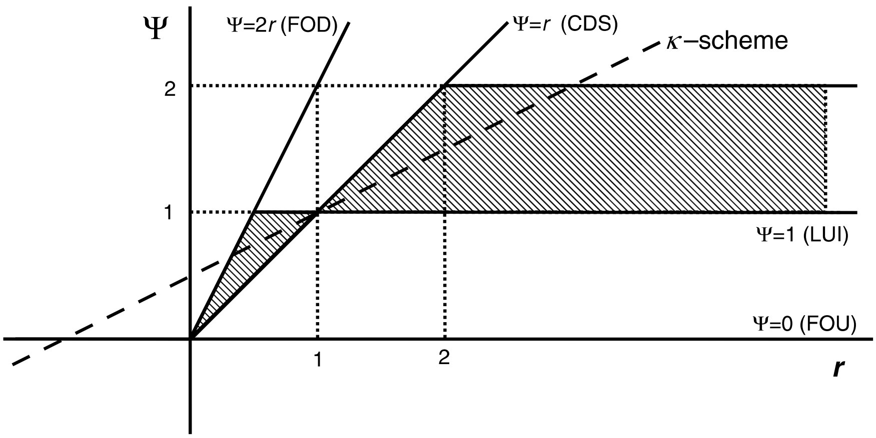

Fig. 2. Flux-limiter diagram: Sweby second-order TVD region and κ-schemes.

3.2. Boundedness criteria

The ideal limiter function should achieve fully bounded behaviour in the solution without compromising the accuracy achieved by the best linear schemes. In order to achieve the desired bounded behaviour, limiter functions are designed to fulfill particular boundedness criteria, usually either the *total-variation diminishing* (*TVD*) [16,46,47] or *positivity* [43,44] conditions.

3.2.1. Total-variation diminishing

The total-variation diminishing or TVD concept was introduced by Harten [16] and translated by Sweby [46,47], in the context of an explicit time discretization, into a set of limitations on the behaviour of a flux-limiter function:

$$0 \leqslant \Psi(r) \leqslant \min(2r, 2), \quad r \geqslant 0 \quad \text{and} \quad \Psi(r) = 0, \; r \leqslant 0, \tag{14}$$

which define a region in the flux-limiter diagram. Note that the second condition does not arise directly from the TVD requirement but is added as a safe treatment for extrema. Sweby also combined the area swept out by the full range of κ-schemes with the TVD region to create a region in the FL diagram, shown in Fig. 2, within which schemes can be both second order and TVD. Roe [39] considered a semi-discrete form and derived the TVD condition $\Psi(r) \leqslant \max(0, 2r)$ for the spatial discretization (ignoring any time-step restrictions).

Roe [3,38] has shown that in the context of explicit time-varying schemes a weaker set of conditions can be employed, depending upon the local Courant number. Goodman and Leveque [15] showed that on general grids in two space dimensions TVD schemes cannot be more than first order, though, as noted by Leveque [28], this does not prevent one-dimensional TVD schemes being applied quite successfully in multiple dimensions through the use of "dimensional splitting" along individual grid directions, though such schemes are not technically TVD.

3.2.2. Positivity

More flexible boundedness criteria can be derived by separating the space and time discretizations and replacing the TVD concept with more general conditions on the coefficients of the nodal discretization (2). Patankar [34] argued on physical grounds that a discretization of the form (2) should have the property that the coefficients 'a' should all be of the same sign. This property, referred to in general as *positivity*, is possessed by FOU but not by any of the κ-schemes. Jameson [19,20] has shown that when the same requirement is placed on the semi-discretization of a general scalar, hyperbolic conservation law, with a compact stencil consisting only of immediate neighbours, it leads to schemes in which local extrema can only diminish (the *local-extremum diminishing* or *LED* property).

Spekreijse [43,44] derived a set of conditions for the monotonicity of a flux-limited, finite-volume scheme of the form (10) on a uniform structured mesh in multiple dimensions. The coefficient of the immediate upwind neighbour in each grid direction is required to be positive (just as in [46,39]), as well as having a uniform upper bound, and Spekreijse defined the following conditions to meet these requirements:

$$\alpha \leqslant \Psi(r) \leqslant M \quad \text{and} \quad -M \leqslant \frac{\Psi(r)}{r} \leqslant 2 + \alpha, \tag{15}$$

where $\alpha \in [-2, 0]$ and $M \in (0, \infty)$ are two constants. These inequalities prescribe a region in the flux-limiter diagram, bounded by straight lines, as shown in Fig. 3. Sweby's TVD region in the FL diagram is entirely contained by Spekreijse's positivity region, for $\alpha = 0$ and $M = 2$, and hence all TVD schemes will also be positive but not necessarily vice versa.

Though the regions of the FL diagram and the condition for linearity preservation remain invariant on non-uniform meshes with the above limiter formulation, it should be noted that the TVD and positivity criteria are affected and the above expressions do not guarantee boundedness in the presence of a varying grid distribution. The issue of achieving boundedness on non-uniform meshes has been considered by Berzins and Ware [7], Holstad [17] and Berger et al. [6].

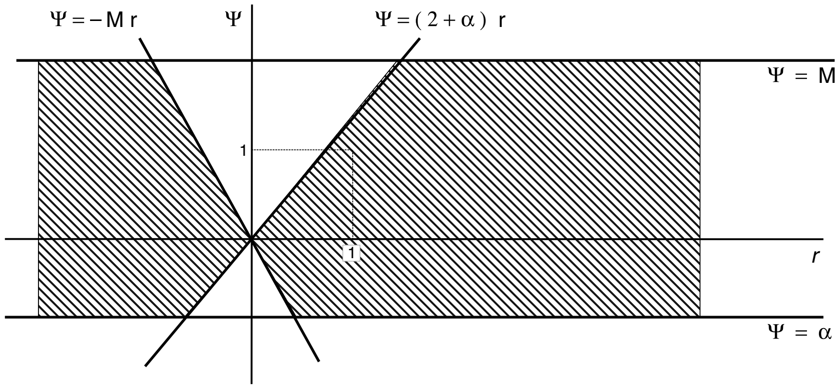

Fig. 3. Flux-limiter diagram: Spekreijse positivity region.

3.3. Classical limiter functions

A number of flux limiter functions have been defined which fulfill some or all of the above criteria, with the majority taking the form either of piecewise-linear functions, ratios of equal-order polynomials or combinations of the two. Some now "classical" limiter functions to be found in standard texts, and all originating from before 1985, are described below and illustrated in Fig. 4. All of these schemes are symmetrical and therefore all are at least tangential to Fromm's scheme at $r = 1$, see Section 5. These limiters can be shown to be representatives of wider classes of schemes, as discussed in Section 6.

3.3.1. Minmod [41]

$$\Psi(r) = \max[0, \min(r, 1)] \quad \text{Minmod} \tag{16}$$

This represents the simple expedient of choosing the shallowest of either the upwind or centred gradients away from extrema and a gradient of zero (*i.e.* first-order upwind) in the presence of extrema (for $r \leqslant 0$). Its behaviour away from extrema can also be interpreted as switching between the CDS and LUI linear schemes and it appears as the lower bound of Sweby's second-order TVD region in the flux limiter diagram, Fig. 2. It is one of the simplest methods for achieving bounded behaviour, though not the most effective, and seems to have been viewed by Roe and Baines [41] mainly as a temporary measure while other possibilities were explored. Its diffusive nature can be understood from the modified equation (8) where it can be seen that the combination of $\kappa = 1$ and -1 in a single cell introduces a local first-order term larger than that for first-order upwind.

3.3.2. Superbee [38]

$$\Psi(r) = \max[0, \min(2r, 1), \min(r, 2)] \quad \text{Supberbee} \tag{17}$$

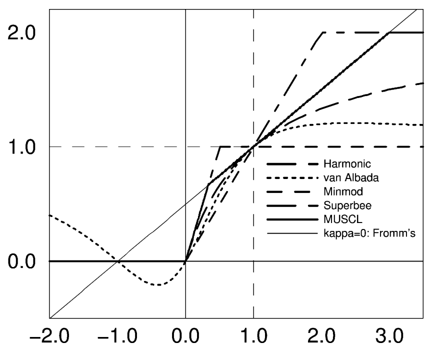

Fig. 4. Flux-limiter diagram: the five "classical" flux limiters.

Superbee appears in the FL diagram as the upper bound of Sweby's second-order TVD region in the flux limiter diagram, Fig. 2. The scheme was designed to achieve the best possible resolution of discontinuities, in which it is very effective, though its extensive use of first-order downwinding ($\Psi(r) = 2r$) in regions of high solution curvature leads to "over-compressive" behaviour in smooth regions, tending for example to square-off smooth extrema. In addition, Superbee, like Minmod, also switches between $\kappa = 1$ and -1 in the smooth region, though in a different combination. This will again tend to introduce a local first-order term of the same size but opposite sign to that for Minmod.

3.3.3. MUSCL [50,51]

$$\Psi(r) = \max\left[0, \min\left(2r, \frac{r+1}{2}, 2\right)\right] \quad \text{MUSCL} \tag{18}$$

van Leer proposed this scheme originally as a slope-limited form of Fromm's scheme, within the context of his variable-extrapolation approach. Converted to FL form, it follows Fromm's scheme as much as possible across Sweby's TVD region, only deviating in regions of high solution curvature or at extrema. It is frequently referred to simply as the "MUSCL" limiter due to its selection in the final MUSCL approach [52], a practice which will be followed here. As will be shown below, it offers an appealing combination of accuracy in smooth flow, reasonable resolution of sharp gradients and the good convergence characteristics associated with Fromm's scheme. This is the only one of the classical limiters which does not introduce the local first-order term of Eq. (8) for smooth solutions (by using only Fromm's scheme in the smooth region). Barth and Jespersen [5] used the same limiter form in their unstructured grid technique.

3.3.4. Harmonic [50,51]

$$\Psi(r) = \frac{r + |r|}{r + 1} \quad \text{Harmonic} \tag{19}$$

This is a smooth function for $r \geqslant 0$ and was again developed by van Leer in the form of a slope limiter based on Fromm's scheme. Though often described as a limited form of Fromm's scheme, it is important to note that, unlike the MUSCL limiter, it reproduces Fromm's scheme only for the single value $r = 1$. It is so named as the slope used for the higher-order correction, (9), is a harmonic average of the centred and upwind gradients. In common with all smooth limiters, the local first-order term, shown in Eq. (8), will be introduced as each value of r is associated with a different κ value (though in general the size of the term will be less than that for Minmod or Superbee).

3.3.5. van Albada [49]

$$\Psi(r) = \frac{r(r+1)}{r^2+1} \quad \text{van Albada} \tag{20}$$

This limiter is smooth, finite and continuous over the entire range of r, which is especially advantageous for fully-implicit implementations, and it tends to one as r tends to $\pm\infty$. It is the only one of the "classical" limiters which does not revert to first-order upwind at extrema ($\Psi(r) = 0$ for $r \leqslant 0$). It therefore does not conform to Sweby's TVD criteria for $r < 0$ but does obey Spekreijse's weaker positivity criteria. It is interesting to note that very few such limiter functions have been proposed since van Albaba, though five smooth, continuous functions, with similar or better performance, most notably the OSPRE limiter, were proposed in [59].

4. Non-linear schemes – normalized-variable approach

The normalized-variable (NV) approach, proposed by Leonard [26,27] and further developed by Gaskell and Lau [14], uses the quantity:

$$\phi_C^* = \frac{\phi_C - \phi_U}{\phi_D - \phi_U} \tag{21}$$

as a gauge of local solution behaviour. Linear schemes may be expressed as linear relationships between the similarly-normalized face value, ϕ_f^*, and ϕ_C^*, which appear as straight lines in the *normalized-variable (NV) diagram*, shown in Fig. 5. As for the FL diagram, various regions can be identified: values of ϕ_C^* between 0 and 1 indicate monotonic variation in the solution while values outside this range indicate the presence of an extremum. Values close to $\phi_C^* = 0$ or 1 indicate strong solution curvature while the value $\phi_C^* = \frac{1}{2}$ indicates a linear variation in the solution for which a normalized face value of $\phi_f^* = \frac{3}{4}$ is required to achieve linearity preservation.

4.1. Boundedness criteria

The most widely referenced boundedness criterion using the NV approach is Gaskell and Lau's *Convection-Boundedness Criterion* (*CBC*) [14] which is based on the premise that for a scheme to produce *computed boundedness* it must possess both *convective stability* (essentially upwind bias) and *interpolative boundedness* (the face value must be bounded by the local cell-centre values). Their CBC appears graphically as a region in the NV diagram, shown in Fig. 5 by the thick black triangle and FOU line, and is violated by all κ-schemes. The CBC requires that if the local solution is monotonic then the predicted face value must fall between the FOU and first-order downwind lines, while if there is an extremum the FOU value must be used. Yu et al. [61] have proposed a modified version of the CBC in NV form which is more restrictive for ϕ_C^* in the range [0,1] but does not impose FOU at extrema. Leonard's original analysis [26,27] was also less restrictive than the CBC at extrema.

4.2. Normalized-variable schemes

NV schemes typically use conditional statements to switch between linear schemes or polynomial curve fits in the NV diagram. Some examples of piecewise-linear NV schemes are: SMART [14], SOUCUP [63] and BSOU [32] while HLPA [64] and SMARTER [9] represent respectively quadratic and cubic curve fits. Leonard's SHARP scheme [27] is unusual in having a more complex functional form and not reverting to FOU at extrema. The Gamma scheme of Jasak et al. [21] is a bounded form of CDS with a parameter controlling the resolution of discontinuities (see Section 6.5).

It should be noted that three of the above NV schemes: SOUCUP, BSOU and HLPA are identical to earlier flux-limited schemes, expressed as in (10), respectively: Minmod, Chakravarthy–Osher (for $\alpha = 0$) [8] and Harmonic. The cubic fit used in SMARTER, which in common with most NV schemes is tangential to QUICK, has been published at least four times under different names [9,33,62,65], the earliest name being used here (see also Section 6.4.3). In the present work, following the approach adopted in [59], all NV schemes have been converted into more convenient FL forms, facilitating their analysis and classification in Section 6. FL forms of various NV schemes are given in the tables of Appendix A (along with their various aliases).

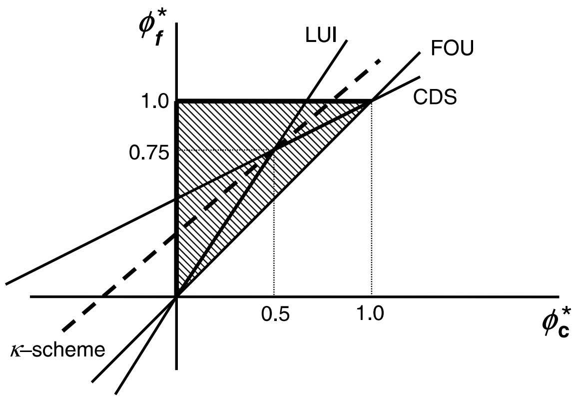

Fig. 5. Normalized-variable diagram: CBC region and κ-schemes.

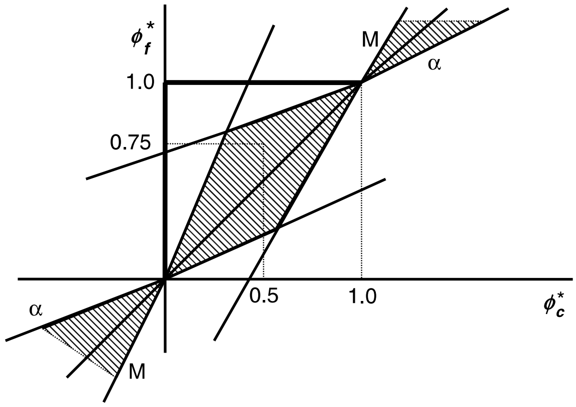

Fig. 6. Normalized-variable diagram: Spekreijse positivity region.

4.3. Relationship to flux-limiter approach

The variable ϕ_C^* is analogous to the gradient ratio, r, and the two are related by the simple expression (for constant grid spacing): $\phi_C^* = 1/(r+1)$, which allows the conversion of NV schemes to FL and vice versa. It also allows the CBC to be compared with the TVD and Positivity boundedness criteria, as described below. It is important to note that in contrast to the gradient ratio, r, ϕ_C^* is fundamentally a ratio of *differences* which means that for non-uniform meshes the form of the NV diagram changes with the geometry of the mesh, in particular the location of the critical point required for linearity preservation $(\frac{1}{2}, \frac{3}{4})$. The approach can be applied to non-uniform meshes via a transformation back to a uniform mesh [12,21] but this increases the complexity of the resulting NV schemes.

4.4. Comparison of boundedness criteria

As shown in [58,59], Spekreijse's positivity region in the FL diagram can be transformed into the NV diagram, Fig. 6. The region produced is controlled by four straight lines whose gradients are functions of α and M. If the CBC is translated into FL form it is similar to Sweby's TVD criteria but with an infinite maximum bound, *i.e.* $M = \infty$. This results from the infinite slope permissible in the ϕ_f^* curve in the NV diagram at $\phi_C^* = 0$. The CBC is therefore weaker than TVD for $r \geqslant 0$ but equivalent to TVD and stronger than positivity for $r \leqslant 0$. Hence TVD $\Rightarrow$ CBC $\Rightarrow$ positivity but not vice versa. The modified CBC of Yu et al. [61] is similar in form but less flexible than the positivity conditions. In practice most positive schemes will also fulfill the CBC with the exception of smooth continuous limiters such as van Albada which do not respect $\Psi(r) = 0$ for $r \leqslant 0$.

5. Design principles for non-linear schemes

This section considers two essential and five optional properties which non-linear convection schemes can be designed to achieve. While the two essential properties are shared by almost all published schemes, the optional properties help to distinguish those schemes which are more or less successful in practice. The two essential properties are listed first.

5.1. Boundedness

This is the property of not producing unphysical spatial oscillations in the solution, including under/overshoots of physical limits on variables, which is not possessed by any linear scheme of greater than first-order accuracy. As discussed in Section 3.2, Spekreijse's positivity conditions give a flexible and general criterion for achieving boundedness and for this reason will be preferred here over the TVD and CBC conditions also outlined above. A scheme will be classed as positive if its limiter function stays within the Spekreijse positivity region, shown in Fig. 3.

5.2. Linearity preservation

This is achieved by ensuring that $\Psi(1) = 1$ which signifies that the scheme will respect exactly a linear variation in the solution, which occurs for $r = 1$. On a uniform mesh this also implies second-order accuracy. The region around $r = 1$ represents smooth monotonic variation in the solution and therefore most areas of typical flow solutions away from discontinuities and extrema. It is in this region that it is most important to ensure that a κ-scheme with desirable properties is active. Only schemes fulfilling this condition will be considered here.

Zijlema [66] has also proposed an additional criterion for second-order accuracy at smooth extrema: $3\Psi(\frac{1}{3}) - \Psi(-1) = 2$, though the practical significance of this result remains unclear. This property is fulfilled by all κ-schemes but by few non-linear schemes. For the majority of limiters $\Psi(-1) = 0$ and hence the condition becomes $\Psi(\frac{1}{3}) = \frac{2}{3}$, which is true only for first-order downwind, $\Psi(r) = 2r$, and for Fromm's scheme. A number of schemes revert to $\Psi(r) = 2r$ as r approaches zero but most for $r < \frac{1}{3}$. Two exceptions, which therefore fulfill the condition, are MUSCL and Superbee, though as noted above Superbee cannot be recommended for resolving smooth extrema. (Two members of the GPL-κ-max class presented below, HOAB [60] and VONOS [54], which behave identically to MUSCL and Superbee respectively for $r < 1$, also meet the criterion.)

5.3. Symmetry

A scheme is symmetric if the averaging function $B(p,q)$ in Eq. (9) gives equal weight to both gradients, *i.e.* $B(p,q) = B(q,p) \Rightarrow \Psi(r) = r\ \Psi(1/r)$. The only symmetric κ-scheme is Fromm's scheme ($\kappa = 0$) to which all symmetric limiters will be tangential at $r = 1$. All of the "classical" limiters listed above in Eqs. (16)–(20) are symmetric. It is possible that the appealing convergence properties of Fromm's scheme, found in [58] and outlined above, may be associated with the symmetry property and these appear to be shared by the various symmetric limited schemes. For a symmetric scheme $\Psi'(0) = M$, the maximum bound, and hence, as $\Psi'(0) \leqslant (2 + \alpha)$ for positivity, this results in the condition: $M \leqslant 2 + \alpha$ and M therefore cannot be greater than 2 in the case of symmetry.

5.4. Smooth-flow target scheme

It may be considered desirable to design a limiter that reverts to a particular linear scheme in smooth flow, *i.e.* for $r \approx 1$. In this case the goal will be to specify the gradient $\Psi'(1) = (\kappa + 1)/2$ for some κ-scheme. If the limiter has been chosen to be symmetric then $\Psi'(1) = \frac{1}{2}$, though this may only be an average of two κ-schemes with the property $\kappa_1 = -\kappa_2$.

5.5. Second derivative at r = 1

It is important that the amount of switching in the sensitive $r = 1$ region should be minimized, preferably by using one κ-scheme for $r \approx 1$. Switching across $r = 1$ can lead to the use of non-optimal or mixed κ-schemes over large parts of the solution domain, reducing solution accuracy, and can affect convergence behaviour under some conditions due to non-linear switching between schemes or "limiter chatter". As noted in Section 2.2, use of mixed κ-schemes introduces a localized first-order term, as in Eq. (8). It was found in [58] that convergence of both the Minmod and Superbee schemes applied to a laminar, incompressible shear-driven cavity problem suffered from oscillations associated with discontinuous switching of schemes across $r = 1$ at certain locations in the flow field, and therefore required greater under-relaxation. As a result the convergence times for Minmod and Superbee were more than 100% greater than those of the Harmonic or van Albada limiters (in addition to giving less accurate results).

5.6. Gradient at r = 0: $\Psi'(0)$

In order to achieve interpolative boundedness it is required that $\Psi'(0) \leqslant (2 + \alpha)$, where $-1 \leqslant \alpha \leqslant 0$, while in order to remain within the κ-scheme region it is also required that $\Psi'(0) \geqslant 1$. $\Psi(r) = 2r$ is the first-order *downwind* scheme and $\Psi(r) = r$ is central differencing, hence $\Psi'(0)$ controls the amount of downwinding used to preserve discontinuities of negative curvature. While excessive use of first-order downwinding leads to over-compressive behaviour, *e.g.* squaring off smooth extrema (as in the case of Superbee) its use in cases of extreme curvature, *i.e.* for r very close to zero, can be recommended for effective resolution of discontinuities. In the case of limiters designed to be smooth and continuous over the full range of r, such as van Albada, α must be finite and less than zero and $\Psi'(0)$ must be less than 2. This indicates that smooth continuous limiters must compromise resolution of sharp gradients compared to the best non-smooth limiters, in particular if, as in the case of van Albada, there is also a low maximum bound (see property 5.7).

5.7. Maximum bound: $\Psi(r) \leqslant M$, as $r \to \pm\infty$

A larger value of M can give better resolution of sharp gradients but may require heavier relaxation, or shorter time steps in unsteady problems. Typically: $1 \leqslant M \leqslant 4$. (There may exist $\Psi(r) > M$ at local maxima.) In the case of symmetry, $\Psi'(0) = M$, and hence the maximum bound and gradient at zero cannot be chosen independently.

6. Classification and analysis of non-linear schemes

A limited number of classes of non-linear schemes have been identified and are presented here, encompassing most of the effective schemes so far proposed. This classification also facilitates examination of the properties of each of these classes and the relative performance of the various schemes. Transformation of the NV schemes considered into the more convenient FL form allows these to be included in the analysis. The tables given in Appendix A summarize all of these classes along their various members and the properties of each of the schemes: smooth-flow target scheme, maximum bound and slope at $r = 0$.

Most limiter formulations of interest fall into two basic categories:

(a) *Piecewise-linear* (*PL*) *functions* which offer the advantage of great flexibility, act simply as switches between linear schemes. In this way, bounded versions of existing linear schemes may be produced. The disadvantage is that its discontinuous nature may have adverse effects upon convergence behaviour under some circumstances, in particular with a fully-implicit implementation. All PL schemes considered here revert to first-order upwind ($\Psi(r) = 0$) at extrema ($r < 0$).

(b) *Polynomial ratios* (*PR*) which offer the possibility of constructing smooth, continuous limiter functions without discontinuous switching. The main disadvantages are lack of flexibility and difficulty of design and lower accuracy than the best PL schemes, due to the use of a mixture of κ-schemes. In this study the starting point was the most general possible polynomial ratio which was examined in particular for ratios of polynomials of order $n = 1$ and $n = 2$, applying the various properties 5.1 to 5.7.

6.1. Symmetric piecewise-linear (SPL) schemes

The simplest symmetric piecewise-linear limiter is MUSCL which simply follows Fromm's scheme for $r \approx 1$, only deviating to remain with the symmetric TVD region. All other symmetric PL limiters must switch κ-schemes across the $r = 1$ point, in a symmetric combination, κ_1 and κ_2, for which $\kappa_1 = -\kappa_2$. The earliest examples of this are Minmod and Superbee which both switch between $\kappa = 1$ and -1 (CDS and LUI respectively) across $r = 1$, the former using CDS for $r \leqslant 1$ and the latter for $r \geqslant 1$.

Most symmetric piecewise-linear limiters can therefore be grouped into two classes, termed here SPL-min and SPL-max, for which the respective classical archetypes are Minmod and Superbee (with MUSCL being a degenerate member of both classes):

$$\Psi(r) = \max\left[0, \min\left\{Mr, \frac{1}{2}(1+\kappa)r + \frac{1}{2}(1-\kappa), \frac{1}{2}(1-\kappa)r + \frac{1}{2}(1+\kappa), M\right\}\right] \quad \text{SPL-min} \tag{22}$$

and

$$\Psi(r) = \max\left[0, \min\left\{Mr, \max\left(\frac{1}{2}(1+\kappa)r + \frac{1}{2}(1-\kappa), \frac{1}{2}(1-\kappa)r + \frac{1}{2}(1+\kappa)\right), M\right\}\right] \quad \text{SPL-max} \tag{23}$$

for which $1 \leqslant M \leqslant 2$. The key distinction is that in the SPL-min limiters the slope decreases with increasing r, across $r = 1$, while for the SPL-max class it increases.

Examples of SPL-min limiters are Minmod ($\kappa = 1$, $M = 1$), MUSCL ($\kappa = 0$, $M = 2$), UMIST [29] ($\kappa = \frac{1}{2}$, $M = 2$) and SPL-$\frac{1}{3}$ [59] ($\kappa = \frac{1}{3}$, $M = 2$). The only published examples of SPL-max limiters of which the present authors are aware are Superbee ($\kappa = 1$, $M = 2$) and MUSCL once again. Other obvious members of the class would be SPL-max-$\frac{1}{2}$ ($\kappa = \frac{1}{2}$, $M = 2$) and SPL-max-$\frac{1}{3}$ ($\kappa = \frac{1}{3}$, $M = 2$) which might be worthy of investigation as less severe alternatives to Superbee. They would be expected to have behaviours falling between those of the MUSCL and Superbee schemes and might show a tendency towards over compression. The Superbee scheme, exemplifying the SPL-max class, can be seen in Fig. 4 while the SPL-$\frac{1}{3}$ scheme, representing the SPL-min class, is shown in Fig. 7. Table A2 summarizes the details of these two classes and their various members.

With the exception of MUSCL, all SPL schemes violate property 5.5 in that they switch κ-schemes across $r = 1$. This can affect convergence behaviour under some circumstances and tends to lead to the use of non-optimal κ-schemes over part of the solution field (*e.g.* $\kappa = -\frac{1}{2}$ or $-\frac{1}{3}$) and even combinations of two different linear schemes in the same cell. As already noted above, the use of mixed κ-schemes tends to introduce a localized first-order term, shown in Eq. (8), which in this case would have a coefficient of $\pm\kappa$.

6.2. Generalized piecewise-linear (GPL) schemes

Removal of the requirement for symmetry allows a more flexible definition of piecewise-linear schemes. An important class arises from the simple expedient of using a single chosen κ-scheme to traverse the positive region of the FL diagram for $r > 0$, combined with a maximum bound, M, and downwind-influence parameter, α, for regions of high solution curvature, controlling $\Psi'(0)$. This has its origins in the van Leer MUSCL scheme and was considered by Hunsdorfer et al. [18] (who assumed $M = 2$ and $\alpha = 0$). The class, termed here GPL-κ, can be expressed as:

$$\Psi(r) = \max\left[0, \min\left\{(2+\alpha)r, \frac{1}{2}(1+\kappa)r + \frac{1}{2}(1-\kappa), M\right\}\right], \quad \text{GPL-}\kappa \tag{24}$$

where $M \geqslant 1$ and $-1 \leqslant \alpha \leqslant 0$.

In addition to MUSCL ($\kappa = 0$, $M = 2$, $\alpha = 0$) it also includes two other schemes of interest: Koren's limited CUI scheme ($\kappa = \frac{1}{3}$, $M = 2$, $\alpha = 0$) and the FL form of Gaskell and Lau's SMART scheme ($\kappa = \frac{1}{2}$, $M = 4$, $\alpha = 0$), defined originally in NV form as a bounded QUICK scheme. It also contains two further schemes of less practical interest: the Chakravarthy–Osher limiter [8] ($\kappa = -1$, $M = 1$), which includes the NV scheme BSOU [32] for $\alpha = 0$ and represents a bounded linear-upwind scheme, and a bounded central-difference

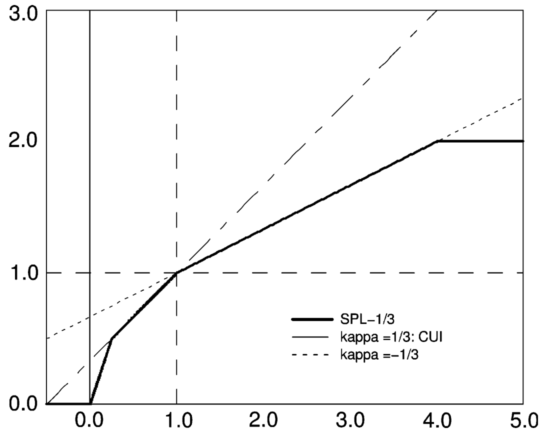

Fig. 7. Example of symmetric piecewise-linear (SPL-min) limiter: SPL-$\frac{1}{3}$.

scheme, BCDS ($\kappa = 1$, $M \geqslant 1$, $\alpha = -1$) [59]. The resolution of discontinuities improves with increasing values of M and decreasing values of $|\alpha|$, however larger values of M tend to have a negative effect on convergence behaviour so an optimum value needs to be chosen (usually in the range 2–4). The MUSCL and SMART schemes are shown in Fig. 8. Table A3 summarizes the details of this class and its various members.

The Koren CUI limiter is very similar in principle to a limited $\kappa = \frac{1}{3}$ scheme proposed by Roe and Baines [41], and further investigated by Arora and Roe [3], in the context of explicit space-time discretizations. The above form is a very convenient implementation of SMART as it requires neither multiple conditional statements nor the special under-relaxation practices described in [14]. As noted in [59], the convergence behaviour of SMART may be enhanced by reducing M from 4 to 2 or 3, with only a slight effect on the resolution of discontinuities. A number of minor modifications to SMART, altering either M, α or both, have been published in NV form under a confusing variety of names (listed in Table A3).

6.3. Symmetric polynomial-ratio (SPR) schemes

Considering the rather restricted class of PR limiters fulfilling the symmetry property, the only PR expression of power $n = 1$, satisfying properties 5.1 to 5.3 is:

$$\Psi(r) = \frac{2r}{r+1}, \tag{25}$$

which is in fact the van Leer Harmonic expression, (19), for $r \geqslant 0$. In the NV formulation, this expression is equivalent to fitting a quadratic curve through the three critical points (0,0), $(\frac{1}{2}, \frac{3}{4})$ and (1,1) in the NV diagram.

Selecting $n = 2$ leads to a one-parameter class of smooth limiters, controlled by M:

$$\Psi(r) = \frac{Mr(r+1)}{r^2 + 2(M-1)r + 1}, \quad 1 \leqslant M \leqslant 1.5. \tag{26}$$

$M = 1$ recovers the van Albada expression (20), however a new limiter is given by the limiting case of $M = 1.5$. This makes much fuller use of the positivity region than does van Albada, with a larger value of M (and $\Psi'(0) = M$) leading to better resolution of sharp gradients. As symmetric ratios for $n = 3$ always factorize back to $n = 2$, this limiter, proposed by the present authors in [59], was termed the *Optimum Symmetric Polynomial-Ratio Expression* or *OSPRE*:

$$\Psi(r) = \frac{3r(r+1)}{2(r^2 + r + 1)}, \quad \text{OSPRE} \tag{27}$$

The van Albada and OSPRE schemes are shown in Fig. 9 and Table A4 summarizes the details of the two schemes.

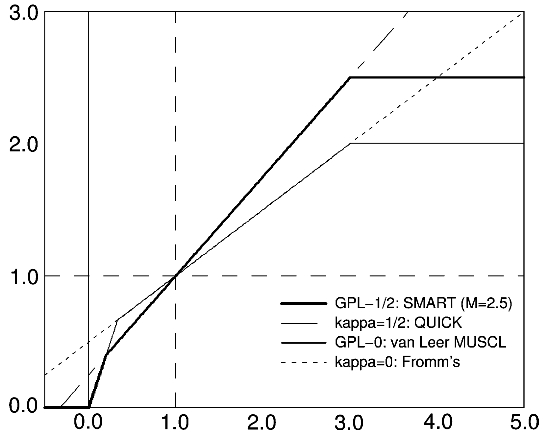

Fig. 8. Examples of generalized piecewise-linear (GPL-κ) limiters.

6.4. Generalized polynomial-ratio (GPR) schemes

It is clear from the above that symmetry represents a very tight restriction on limiter design and its removal allows the specification of the other properties, in particular the choice of a target κ-scheme. A general two-parameter class of PR limiters allowing the specification of a target κ-scheme and a maximum positive bound, M, can be defined as follows:

$$\Psi(r) = \frac{r(Mr+\beta)}{r^2+(M-1)r+\beta}, \quad \beta = \frac{2}{1-\kappa} - M \geqslant 0. \quad \text{GPR-}\kappa \tag{28}$$

Some members of the class are smooth and continuous over the full range of $r \in (-\infty, +\infty)$, under the necessary condition $(M-1)^2 < 4\beta$, while the rest are well-defined only for $r \geqslant 0$. Most have order 2 and the slope property: $\Psi'(0) = 1$, though for $\beta = 0$ they factorize down to order 1 with $\Psi'(0) > 1$. The class includes most of the interesting PR limiters so far published, including the Harmonic and van Albada schemes. It should be noted that not all combinations of M and κ in (28) yield positive schemes and some necessary but not sufficient conditions for positivity are given in Table A4.

In each of the cases: $\kappa = 0, \frac{1}{3}$ and $\frac{1}{2}$, the class leads to at least three types of limiters: a van Albada type (for $M = 1$), a Harmonic type (for $\beta = 0$) and a further smooth, continuous form (for $M = 2$, $\kappa > 0$ and $M = \frac{3}{2}$, $\kappa = 0$). The van Albada and Harmonic types form sub-classes and are considered in the two following sub-sections which are followed by consideration of a further class of PR limiters converted from cubic polynomials in the NV diagram and of which one member, for $\kappa = \frac{1}{2}$, also belongs to the GPR class. Fig. 10 shows examples of smooth, continuous GPR-κ schemes while Fig. 11 shows examples of the harmonic-type. Tables A4 and A5 summarize the details of these classes, for continuous and discontinuous functions respectively.

6.4.1. Generalized van Albada (GVA) schemes

The case of $M = 1$ leads to a generalized class of van Albada limiters, identified in [59], which share with van Albada the properties $M = 1$ and $\Psi'(0) = 1$ but have been designed to be tangential to specific κ-schemes:

$$\Psi(r) = \frac{r(r+\beta)}{r^2+\beta}, \quad \beta = \frac{1+\kappa}{1-\kappa}, \quad \text{GVA-}\kappa \tag{29}$$

These share with van Albada and OSPRE the property that for $r = -1$, at symmetrical extrema, they revert to their target schemes. The van Albada and GVA-$\frac{1}{2}$ limiter functions are shown in Fig. 10 and the GVA-κ schemes are summarized in Table A4.

6.4.2. Generalized harmonic (GH) schemes

In the case of $\beta = 0$ the GPR-κ limiters factorize down to order 1, leading to a generalized form of the Harmonic limiter identified by the present authors in [59] and termed there "generalized harmonic". This is a one-parameter class defined using M, the maximum bound, and smooth only for $r \geqslant 0$:

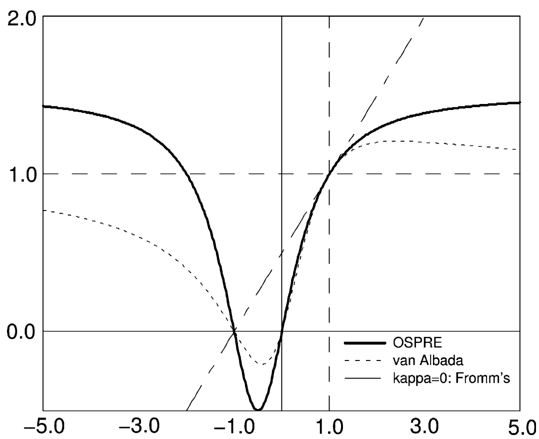

Fig. 9. Examples of symmetric polynomial-ratio (SPR) limiters.

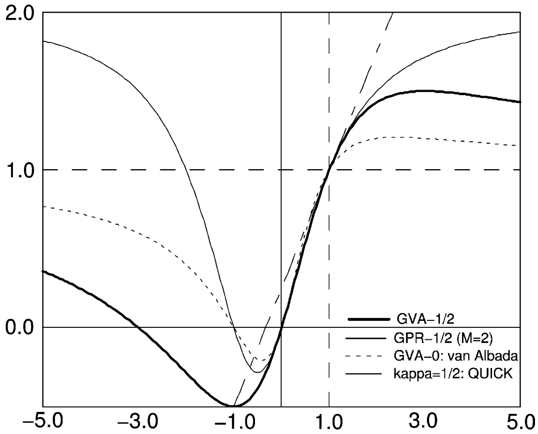

Fig. 10. Examples of generalized PR (GPR-κ) and van Albada (GVA) limiters.

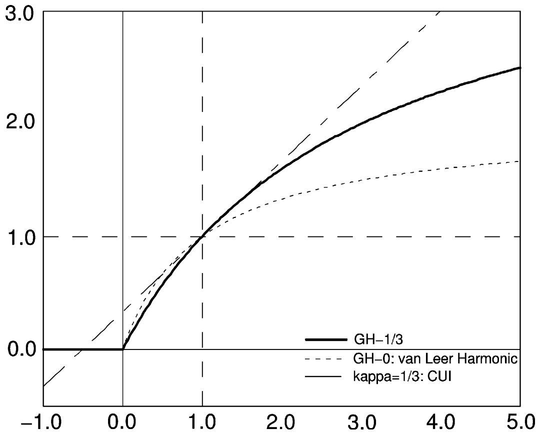

Fig. 11. Examples of generalized harmonic (GH-κ) limiters.

$$\Psi(r) = \frac{M(r+|r|)}{2(r+M-1)}, \quad M = \frac{2}{1-\kappa} \geqslant 2, \quad \text{GH-}\kappa \tag{30}$$

for which $\Psi'(0) = M/(M–1)$. $M = 2$ gives van Leer Harmonic ($\kappa = 0$, $\Psi'(0) = 2$), $M = 3$ gives H-CUI [59] $\kappa = \frac{1}{3}$, $\Psi'(0) = 1.5$) and $M = 4$ gives H-QUICK [59] ($\kappa = \frac{1}{2}$, $\Psi'(0) = 1.33$). The van Leer Harmonic (GH-0) and H-CUI (GH-$\frac{1}{3}$) schemes are shown in Fig. 11 and the GH-κ schemes are summarized in Table A5.

6.4.3. Polynomial NV schemes

A number of schemes have been proposed using simple polynomial functions to traverse the CBC region of the NV diagram, passing through the three critical points: $(0,0)$, $(\frac{1}{2}, \frac{3}{4})$ and $(1,1)$. Such polynomials in NV form, of order n, transform into polynomial-ratio limiters of order $(n-1)$ in FL form. Zhu [64] proposed a quadratic fit, HLPA, which is equivalent to the Harmonic limiter in FL form (tangential to Fromm's scheme) while a number of authors [9,33,62,65] have proposed the same cubic polynomial, tangential to QUICK at $\phi_C^* = \frac{1}{2}$, under a variety of names (it will be referred to here as SMARTER). This can be generalized to a wider class of polynomials [66] each tangential to a specific κ-scheme which can be written in the following FL form which is smooth for $r \geqslant 0$:

$$\Psi(r) = \frac{(r+|r|)\{(1+\kappa)r + (1-\kappa)\}}{(r+1)^2}, \quad 0 \leqslant \kappa \leqslant 1, \ \text{PNV} - \kappa \tag{31}$$

for which $M = 2(1+\kappa)$ and $\Psi'(0) = 4 - M$. This reduces to the Harmonic limiter for $\kappa = 0$ ($M = 2$, $\Psi'(0) = 2$), gives a limiter tangential to $\kappa = \frac{1}{3}(M = \frac{8}{3}, \Psi'(0) = \frac{4}{3})$ and gives the SMARTER scheme for $\kappa = \frac{1}{2}$

($M = 3$, $\Psi'(0) = 1$). SMARTER is also a member of the GPR-κ class given above. The PNV-κ schemes are summarized in Table A5.

6.5. Other miscellaneous non-linear schemes

Listed in Table A6 of Appendix A are a number of miscellaneous limiter forms which do not fit into the above classifications for various reasons. Some of these illustrate, by negative example, the benefits of following the proposed design principles.

In [59] a quadratic curve fit in the FL diagram, GPa-κ, was suggested with a single parameter, κ, defining the target κ-scheme and setting the slope at $r = 0$. The performance of the GPa-$\frac{1}{2}$ scheme was examined in [59] and shown to be reasonable but not outstanding. Cubic and higher polynomial curve fits allow more parameters to be specified but tend to suffer from inflection points and other irregularities.

Jameson's α-mod scheme [19] is a one-parameter symmetric family giving Minmod for $\alpha = 0$, Harmonic for $\alpha = 1$ and averages of the two in between. These schemes can therefore not be expected to be better than Harmonic and may be considerably worse for low values of α. Jameson's α–β-mod scheme [19] gives α-mod for $\beta = 1$ and $\Psi(r) = \max(0, r^{1/2})$ for $\beta = 0$. For all cases with $\beta < 1$ it gives a maximum bound and $\Psi'(0)$ of ∞ and is therefore not positive for these values.

Spekreijse [43] proposed a one-parameter class of smooth, continuous PR limiters based on κ. These share the properties: $M = 1 + \kappa$ and $\Psi'(0) = 1 - \kappa$ and thus for $\kappa > 0$, $\Psi'(0) < 1$ and for $\kappa < 0$, $M < 1$. For $\kappa \neq 0$ the limiters therefore go partially outside the κ-scheme region (using a convex average of CDS and FOU). Hence the optimum member of the class is $\kappa = 0$ which is in fact the van Albada limiter. Two other smooth, continuous PR limiters, of Spekreijse [43] and Koren [23] respectively, are included in Table A6, both of which share the problem of having $\Psi'(0) = \frac{1}{2}$ and therefore going outside the κ-scheme region.

The Gamma scheme of Jasak et al. [21], proposed in NV form as a modified form of CDS respecting the CBC, blends CDS with an ad hoc quadratic function. The blending is controlled by a parameter, β_m, recommended to fall in the range 0.1–0.5, with lower values giving better resolution of sharp gradients and higher values giving better convergence. In FL form it can be seen to be a combination of CDS with a polynomial ratio of order 1, with β_m being equal to the reciprocal of the maximum bound, M. For $M = 2$ ($\beta_m = 0.5$) it is equivalent to a blending of the Minmod (for $r \leqslant 1$) and Harmonic ($r \geqslant 1$) limiters while as M increases it becomes closer to bounded CDS [59] which uses CDS ($\kappa = 1$) over most of the smooth region and can require heavy under-relaxation, see Section 7.2. Jasak et al. [21] give results for $\beta_m = 0.1$ ($M = 10$) which are close to the accuracy of the SMART scheme for smooth extrema and sharp gradients (though at the expense of the problematic convergence associated with CDS), while Alves et al. [2] show results using $\beta_m = 0.5$ which are only slightly better than those for Minmod (as would be expected from the above analysis).

Table A6 also contains several other limiters whose complex functional forms or unusual characteristics render them less interesting for practical use.

7. Numerical implementation and comparison

In [58,59] a number of schemes were implemented within the PHOENICS CFD code [45], which solves the Reynolds-averaged Navier–Stokes equations using a staggered, cell-centred, finite-volume discretization and a version of the SIMPLE pressure-correction algorithm. All solutions here were obtained using a version of Stone's strongly-implicit algorithm [34]. The implementation was carried out using a deferred-correction approach via source terms [22,58]. All non-linear schemes considered were expressed in the form of flux limiters, thereby allowing direct comparison free of implementational differences and enhancing program synergy.

7.1. Scalar advection test cases

General comparisons were described in [58] using several standard incompressible, viscous test cases however attention here will be restricted to two steady, 2D scalar convection cases considered in [59]. These are both based on the circular velocity field: $u(x,y) = y$ and $v(x,y) = -x$ in a rectangular domain $x \in [-1, 1]$

and $y \in [0,1]$. Non-zero inflow values are specified only for $x \in [-1,0]$ and $y = 0$ where one of two profiles is imposed, the first smooth, the second discontinuous:

- *Case 1* – Gaussian distribution: $\phi(x) = \exp(-2x)\sin^2(\pi x)$.
- *Case 2* – three-level step function: $\phi(x) = 0$, $x < 0.2$ or $x > 0.8$, $\phi(x) = 1$ for $0.2 \leqslant x \leqslant 0.4$ and $0.6 \leqslant x \leqslant 0.8$ and $\phi(x) = 0.5$, $0.4 < x < 0.6$.

The exact solutions, $\phi(r)$, consist of the above inlet expressions with $r = \sqrt{(x^2 + y^2)}$ replacing x.

The results for 26 linear and non-linear schemes are given in Table B1 in terms of the number of iterations required for convergence, the false time-step size required and the L_1-norm error in the converged solution. The effective order of accuracy for the smooth solution in Case 1 is also given. The solution fields for the two cases are illustrated in Figs. 12 and 13, respectively, in the form of contours of the scalar field (calculated using the $\kappa = \frac{1}{3}$ scheme for Case 1 and Superbee for Case 2). Figs. 14 and 15 show plots of three solution profiles at the outlet for each of the cases: the most accurate, least accurate and median results. (For Case 2, Superbee is in fact the most accurate scheme but is not plotted due to its lack of general applicability.)

It should be noted that though the implementation is typical of that used in many cell-centred finite-volume computer codes, the relative convergence behaviour of the various schemes may depend on the specific solution procedure employed (for example the use or not of deferred correction) and thus the convergence results presented here cannot be viewed as completely general. The convergence behaviour of non-linear schemes within implicit solution procedures is also considered by Venkatakrishnan [55,56] and Tiesinga [48].

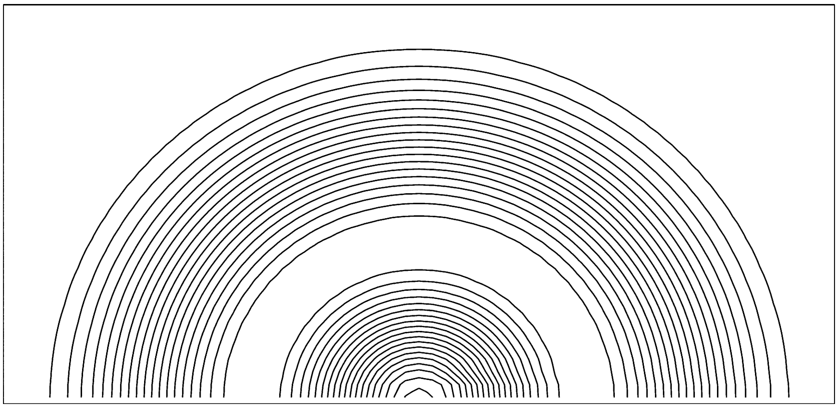

Fig. 12. Gaussian test case – scalar contours for $\kappa = \frac{1}{3}$ scheme.

Fig. 13. Step test case – scalar contours for Superbee scheme.

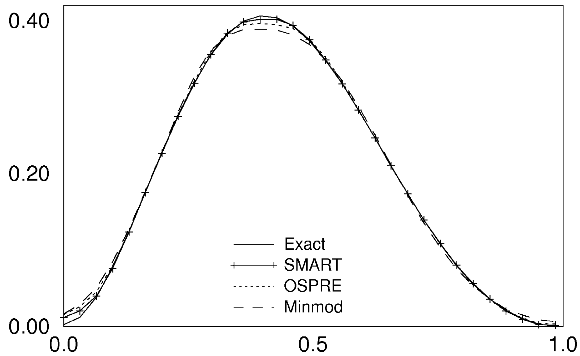

Fig. 14. Gaussian test case (61 × 31 grid) – outlet profiles for three schemes.

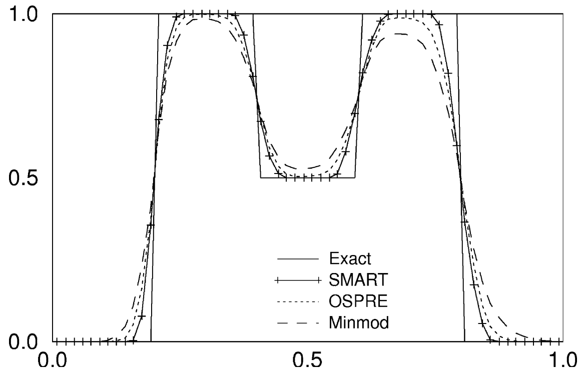

Fig. 15. Step test case (81 × 41 grid) – outlet profiles for three schemes.

7.2. Performance comparisons

In Table B1, the schemes have been placed in an order based on their average ranking (linear and non-linear separately) according to five different measures: *absolute error* and *number of iterations* for Cases 1 and 2 and the *order of accuracy* for Case 1. A score consisting of the normalized averaged ranking (maximum value 1) gives some measure of their relative effectiveness in terms of both accuracy and convergence. Three of the top five schemes (OSPRE, H-CUI and SPL-$\frac{1}{3}$) were proposed in [59] and designed using the principles outlined in Section 5.

The most accurate results for both cases (ignoring Superbee with its special performance for discontinuities in Case 2) were given by the three GPL-κ schemes: MUSCL, SMART and Koren (all in their original forms). These gave error levels and orders of accuracy which were mutually similar but significantly better than other non-linear schemes (with SMART being marginally the most accurate). These three schemes however differ significantly in convergence behaviour with MUSCL requiring less under-relaxation and between 10% and 60% fewer iterations than Koren or SMART and hence being ranked first. SMART (with $M = 4$) requires the highest number of iterations of any scheme for Case 2 and the third highest for Case 1 (though with $M = 2$ it would have somewhat improved convergence, closer to that of the Koren scheme).

Of the "classical" limiters only the van Leer MUSCL and Harmonic schemes appear in the upper half of the ranking. Minmod and Superbee are the least accurate schemes for the smooth case, confirming the analysis in Section 3.3, based on Eq. (8). For the discontinuous case Minmod is the least accurate and Superbee the most accurate.

Of the smooth limiters, the OSPRE scheme, Eq. (27), stands out, giving the best convergence of any scheme in both cases and a reasonable level of accuracy. The H-CUI scheme (smooth for $r \geqslant 0$) also performs well, being more accurate than OSPRE but with slightly slower convergence. The non-symmetric van Albada schemes, GVA-$\frac{1}{2}$ and GVA-$\frac{1}{3}$, though appealing in form, do not improve on the performance of the original van Albada, while the two GPR-κ schemes do slightly better. All of the smooth, continuous limiters, with the exception of OSPRE, appear in the lower half of the ranking.

In general the best convergence results come from the symmetrical schemes, both PL and PR, (with the exception of Superbee) and the worst convergence from the non-symmetric PL schemes. The BCDS scheme gives significantly the worst convergence for the smooth case and, along with SMART, also the worst for the discontinuous case.

8. Conclusions

The flux-limiter and normalized-variable approaches to the design of non-linear convection schemes have been reviewed and compared. The flux-limiter form has been preferred here due to its compactness, flexibility and implementational advantages. Most of the published normalized-variable schemes have been converted to flux-limiter form allowing a general classification and analysis of a large number of schemes within the cell-centred, finite-volume framework. The classification produced is presented in a number of tables which include most published non-linear schemes.

Comparisons of three widely-used boundedness criteria show that Spekreijse's positivity concept gives the most flexible set of conditions, with Gaskell and Lau's Convection Boundedness Criterion (CBC) being more restrictive at extrema and Sweby's total-variation-diminishing (TVD) conditions further adding a lower maximum bound of 2.

A set of properties has been proposed which can be used to design or select non-linear schemes for a particular purpose. Two essential properties, boundedness and linearity preservation, are shared by all schemes of interest, however the remaining five optional properties determine the difference in performance between the various schemes and can be used to understand their behaviour.

Numerical comparisons for two scalar advection cases reveal that the piecewise-linear GPL-κ schemes, SMART, Koren and MUSCL, give the highest, and mutually similar, levels of accuracy. Their convergence behaviour however differs significantly, with MUSCL being the best behaved. Of the smooth, continuous limiters, OSPRE performs the best, combining reasonable accuracy with the best convergence behaviour of any non-linear scheme considered. Of the five "classical" limiter functions considered here: Minmod, Superbee, MUSCL, Harmonic and van Albada, only the MUSCL and Harmonic schemes are competitive with the best of the more recent limiters, with MUSCL being particularly advantageous. The comparisons reveal wide variations in performance between the best and worst schemes, in terms of both accuracy and convergence behaviour, and underline the need to select carefully an appropriate non-linear convection scheme.

Appendix A. Classification of convection schemes

The tables (Tables A1–A6) presented in this appendix attempt to classify all non-linear schemes, of which the authors are aware in the published literature. All schemes have been expressed in flux-limiter form, whether or not they were originally proposed in that form, both for reasons of consistency and for ease of implementation. In all cases, M represents the maximum positive bound of $\Psi(r)$ as $r \to \pm\infty$, $\Psi'(0)$ is the slope of $\Psi(r)$ at $r = 0$ and κ represents the κ-scheme to which the limiter is tangential at $r = 1$ (*i.e.* for a smooth solution).

Table A1
Linear κ-scheme family (unbounded)

Name	Limiter	Reference	Comments
General form	$\frac{1}{2}\{(\mathbf{1}+\boldsymbol{\kappa})\mathbf{r}+(\mathbf{1}-\boldsymbol{\kappa})\}$	**[53]**	**Class of linear schemes: $-1 \leqslant \kappa \leqslant 1$.**
Linear-upwind (LUI)	1	[4,36,57]	$\kappa = -1$: unique fully-upwind κ-scheme.
Fromm	$\frac{1}{2}r + \frac{1}{2}$	[13]	$\kappa = 0$: unique symmetric κ-scheme.
Cubic-upwind (CUI)	$\frac{2}{3}r + \frac{1}{3}$	[1]	$\kappa = \frac{1}{3}$: unique third-order κ-scheme.
Quadratic-upwind (QUICK)	$\frac{3}{4}r + \frac{1}{4}$	[25]	$\kappa = \frac{1}{2}$: unique quadratic interpolation.
Central difference (CDS)	r	–	$\kappa = 1$: unique non-upwind κ-scheme.

Table A2
Symmetric piecewise-linear (SPL) schemes

Name	Limiter	Ref.	κ	M	$\Psi'(0)$	Comments
SPL-min	$\mathbf{max[0, min\{\mathit{M}r, \frac{1}{2}(1+\kappa)r+\frac{1}{2}(1-\kappa), \frac{1}{2}(1-\kappa)r+\frac{1}{2}(1+\kappa), \mathit{M}\}]}$	**[59]**	$\mathbf{[-1,1]}$	$\mathbf{[1,2]}$	$\boldsymbol{M}$	**Symmetric combination of two κ-schemes.**
Minmod	$\max[0,\min(r,1)]$	[41]	$1, -1$	1	1	Also known as: SOUCUP [63].
UMIST	$\max[0,\min(Mr,\frac{1}{4}+\frac{3}{4}r,\frac{3}{4}+\frac{1}{4}r,M)]$	[29]	$\frac{1}{2},-\frac{1}{2}$	$(1,2]$	M	Original: $M=2$.
SPL-$\frac{1}{3}$	$\max[0,\min(Mr,\frac{1}{3}+\frac{2}{3}r,\frac{2}{3}+\frac{1}{3}r,M)]$	[59]	$\frac{1}{3},-\frac{1}{3}$	$(1,2]$	M	Also known as PLS-$\frac{1}{3}$ [59].
MUSCL	$\max[0,\min(Mr,\frac{1}{2}+\frac{1}{2}r,M)]$	[51]	0	$(1,2]$	M	Original: $M=2$. Also known as: MLU [31], Jameson α-mean [19]. Also belongs to SPL-max class.
SPL-max	$\mathbf{max[0, min\{\mathit{M}r, max(\frac{1}{2}(1+\kappa)r+\frac{1}{2}(1-\kappa), \frac{1}{2}(1-\kappa)r+\frac{1}{2}(1+\kappa)), \mathit{M}\}]}$	**Present**	$\mathbf{[-1,1]}$	$\mathbf{(1,2]}$	$\boldsymbol{M}$	**Alternative symmetric combination of two κ-schemes.**
Superbee	$\max[0,\min\{Mr,\max(r,1),M\}]$	[38]	$1, -1$	$(1,2]$	M	Original: $M=2$.
SPL-max-$\frac{1}{2}$	$\max[0,\min(Mr,\max(\frac{1}{4}+\frac{3}{4}r,\frac{3}{4}+\frac{1}{4}r),M)]$	Present	$\frac{1}{2},-\frac{1}{2}$	$(1,2]$	M	
SPL-max-$\frac{1}{3}$	$\max[0,\min(Mr,\max(\frac{1}{3}+\frac{2}{3}r,\frac{2}{3}+\frac{1}{3}r),M)]$	Present	$\frac{1}{3},-\frac{1}{3}$	$(1,2]$	M	
Sweby Φ family	$\mathbf{max[0,min(\mathit{M}r,1),min(r,\mathit{M})]}$	**[46,47]**	$\mathbf{1, -1}$	$\mathbf{[1,2]}$	$\boldsymbol{M}$	**$\Phi \equiv M$. Also known as: Jameson α-bee [19]. Includes Minmod ($M = 1$) and Superbee ($M = 2$).**

Table A3
Generalized piecewise-linear (GPL) schemes

Name	Limiter	Ref.	κ	M	$\Psi'(0)$	Comments
GPL-κ	$\mathbf{max[0, min\{(2+\alpha)r, \frac{1}{2}(1-\kappa)+\frac{1}{2}(1+\kappa)r, \mathit{M}\}]}$	**[18,59]**	$\mathbf{[-1,1]}$	$\geqslant \mathbf{1}$	$\mathbf{2+\alpha}$	**Bounded κ-scheme. $-1 \leqslant \alpha \leqslant 0$.**
Chakravarthy–Osher	$\max[0,\min\{(2+\alpha)r,1\}]$	[8]	-1	$\geqslant 1$	$2+\alpha$	Also known as: BSOU [32] ($\alpha=0$).
MUSCL	$\max[0,\min\{(2+\alpha)r,\frac{1}{2}r+\frac{1}{2},M\}]$	[50,51]	0	$\geqslant 1$	$2+\alpha$	Original: $\alpha=0$, $M=2$. Also known as: MLU [31], Jameson α-mean [19].
Koren	$\max[0,\min\{(2+\alpha)r,\frac{2}{3}r+\frac{1}{3},M\}]$	[24]	$\frac{1}{3}$	$\geqslant 1$	$2+\alpha$	Original: $\alpha=0$, $M=2$. See also: Roe & Baines [41] and Arora & Roe [3].
SMART	$\max[0,\min\{(2+\alpha)r,\frac{3}{4}r+\frac{1}{4},M\}]$	[14]	$\frac{1}{2}$	$\geqslant 1$	$2+\alpha$	Original: $\alpha=0$, $M=4$. Also known as: COPLA ($\alpha=-0.5$, $M=2.5$) [10]; AVL-SMART ($\alpha=-0.5$, $M=2.5$) [37]; CUBISTA ($\alpha=-0.5$, $M=1.5$) [1]; Lin & Lin ($\alpha=0$, $M=2$) [30]; WACEB ($\alpha=0$, $M=2$) [42].
Bounded CDS	$\max[0,\min\{r,M\}]$	–	1	$\geqslant 1$	1	Bounded central-difference scheme. As Minmod for $M=1$.
GPL-κ-max	$\mathbf{max[0, min\{(2+\alpha)r, max(\frac{1}{2}(1+\kappa_1)r+\frac{1}{2}(1-\kappa_1), \frac{1}{2}(1-\kappa_2)r+\frac{1}{2}(1+\kappa_2)), \mathit{M}\}]}$	**Present**	$\mathbf{[-1,1]}$	$\geqslant \mathbf{1}$	$\mathbf{2+\alpha}$	**Combination of two κ-schemes switching across r = 1. $-1 \leqslant \alpha \leqslant 0$.**
Superbee	$\max[0,\min\{(2+\alpha)r,\max(1,r),M\}]$	[38]	-1, 1	$\geqslant 1$	$2+\alpha$	Original: $\alpha=0$, $M=2$.
STOIC	$\max[0,\min\{(2+\alpha)r,\max(\frac{3}{4}r+\frac{1}{4},r),M\}]$	[11]	$\frac{1}{2}$, 1	$\geqslant 1$	$2+\alpha$	Original: $\alpha=0$, $M=4$.
VONOS	$\max[0,\min\{(2+\alpha)r,\max(1,\frac{3}{4}r+\frac{1}{4}),M\}]$	[54]	-1, $\frac{1}{2}$	$\geqslant 1$	$2+\alpha$	Original: $\alpha=0$, $M=18$.
HOAB	$\max[0,\min\{(2+\alpha)r,\max(\frac{1}{2}r+\frac{1}{2},r),M\}]$	[60]	0, 1	$\geqslant 1$	$2+\alpha$	Original: $\alpha=0$, $M=5$.

Table A4
Polynomial-ratio schemes – smooth, continuous functions

Name	Limiter	Ref.	κ	M	Ψ	Comments
Symmetric PR form	$\boldsymbol{Mr(r+1)/(r^2+2(M-1)r+1)}$	**[59]**	**0**	**[1, 1.5]**	$\boldsymbol{M}$	**Symmetry** $\boldsymbol{\Rightarrow \kappa = 0, \Psi'(0) = M}$**.**
van Albada	$r(r+1)/(r^2+1)$	[49]	0	1	1	
OSPRE	$3r(r+1)/2(r^2+r+1)$	[59]	0	1.5	1.5	
Generalized PR-κ	$\boldsymbol{r(Mr+\beta)/(r^2+(M-1)r+\beta)}$	**Present**	**[−1, 1)**	$\boldsymbol{[0, -1+[8/(1-\kappa)]^{1/2})}$	**1**	$\boldsymbol{\beta = 2/(1-\kappa) - M;\ \beta > (M-1)^2/4}$ **(⇒smooth) and** $\boldsymbol{\beta > (M-2)^2/8}$ $\boldsymbol{(\Rightarrow \Psi(r) \leqslant 2r,\ r > 0)}$**.**
GPR-0	$r(3r+1)/(2r^2+r+1)$	Present	0	1.5	1	
GPR-$\frac{1}{3}$	$r(2r+1)/(r^2+r+1)$	[59]	$\frac{1}{3}$	2	1	Also known as: PRNS-$\frac{1}{3}$ [59].
GPR-$\frac{1}{2}$	$2r(r+1)/(r^2+r+2)$	[59]	$\frac{1}{2}$	2	1	Also known as: PRNS-$\frac{1}{2}$ [59].
Generalized van Albada	$\boldsymbol{r(r+\beta)/(r^2+\beta)}$	**[59]**	$[-\frac{7}{9}, \frac{7}{9}]$	**1**	**1**	$\boldsymbol{\beta = (1+\kappa)/(1-\kappa)}$**; GPR-$\kappa$, M = 1.**
van Albada (GVA-0)	$r(r+1)/(r^2+1)$	[49]	0	1	1	$\beta = 1$.
GVA-$\frac{1}{3}$	$r(r+2)/(r^2+2)$	[59]	$\frac{1}{3}$	1	1	$\beta = 2$.
GVA-$\frac{1}{2}$	$r(r+3)/(r^2+3)$	[59]	$\frac{1}{2}$	1	1	$\beta = 3$.

Table A5
Polynomial-ratio schemes – discontinuous functions

Name	Limiter	Ref.	κ	M	$\Psi'(0)$	Comments
Generalized Harmonic	$\boldsymbol{M(r+\lvert r\rvert)/2(r+M-1)}$	**[59]**	**[0, 1)**	$\boldsymbol{2/(1-\kappa)}$	$\boldsymbol{M/(M-1)}$	$\boldsymbol{M \geqslant 2}$**.**
Harmonic	$(r+\lvert r\rvert)/(r+1)$	[50,51]	0	2	2	Also known as: HLPA [64].
H-CUI	$3(r+\lvert r\rvert)/2(r+2)$	[59]	$\frac{1}{3}$	3	$\frac{3}{2}$	
H-QUICK	$4(r+\lvert r\rvert)/2(r+3)$	[59]	$\frac{1}{2}$	4	$\frac{4}{3}$	
Polynomial NV	$\boldsymbol{(r+\lvert r\rvert)[(1+\kappa)r+(1-\kappa)]/(r+1)^2}$	**[66]**	**[0, 1]**	$\boldsymbol{2(1+\kappa)}$	$\boldsymbol{4-M}$	**Cubic polynomial fits in NV diagram.**
PNV-$\frac{1}{3}$	$2(r+\lvert r\rvert)(2r+1)/3(r+1)^2$	[66]	$\frac{1}{3}$	$\frac{8}{3}$	$\frac{4}{3}$	
SMARTER	$(r+\lvert r\rvert)(3r+1)/2(r+1)^2$	[9]	$\frac{1}{2}$	3	1	Also known as: NOTABLE [33], CHARM [62], ISNAS [65].

Table A6
Miscellaneous and hybrid schemes

Name	Limiter	Ref.	κ	M	$\Psi'(0)$	Comments
GPa-κ	$\max[0, \min\{\frac{1}{2}(\kappa-1)r^2 + \frac{1}{2}(3-\kappa)r, M\}]$	[59]	$[-1, 1]$	$[1, (3-\kappa)^2/8(1-\kappa)]$	$(3-\kappa)/2$	Quadratic fit for $r > 0$, BCDS for $\kappa = 1$.
Jameson α-mod	$\max[0, (\alpha+1)r/\{\max(r,1) + \alpha\min(r,1)\}]$	[19]	0	$\alpha + 1$	$\alpha + 1$	$\alpha \in [0, 1]$. Average of Minmod ($\alpha = 0$) and van Leer Harmonic ($\alpha = 1$).
Jameson α–β-mod	$\max[0, (\alpha+1)r^{(\beta+1)/2}/\{\max(r^\beta,1) + \alpha\min(r^\beta,1)\}]$	[19]	0	$[1, \infty)$	$[1, \infty)$	$\alpha \in [0,1], \beta \in [0,1]$. As α-mod for $\beta = 1$. For $\beta < 1$: $\Psi(r) \to (\alpha+1)r^{(1-\beta)/2}$ as $r \to +\infty$ and $\Psi'(r) \to \infty$ as $r \to 0$, *i.e.* not positive. For $\beta = 0$: $\Psi(r) = r^{1/2}$ for $r \geqslant 0$.
Gamma	$\max[0, \min\{r, Mr/(r+1)\}]$	[21]	$\frac{1}{2}$	$\geqslant 2$	1	Original: $2 \leqslant M \leqslant 10$ ($M = 1/\beta_m$).
Spekreijse-κ	$\{(1+\kappa)r + (1-\kappa)\}r/(r^2+1)$	[43]	$[-\frac{1}{3}, 1]$	$1+\kappa$	$1-\kappa$	Gives van Albada for $\kappa = 0$.
Spekreijse	$(\frac{2}{3}r + \frac{1}{3})(3r^3 - 2r^2 + 3r)/2(r^4+1)$	[43]	$\frac{1}{3}$	1	$\frac{1}{2}$	
Koren-PR	$r(2r+1)/(2r^2-r+2)$	[23]	$\frac{1}{3}$	1	$\frac{1}{2}$	$\Psi(r) < r$ for $0 < r < \frac{1}{2}$.
SHARP	$\min[\max\{0, 2r(r^{1/2}-1)/(r-1)\}, \max\{\frac{3}{4}r + \frac{1}{4}, -\frac{5}{4}\}]$	[27]	$\frac{1}{2}$	∞	2	$\Psi(r) \to 1$ as $r \to 1$ but $\Psi(1) = 0/0$. $\Psi(r) \to +\infty$ as $r \to +\infty$, *i.e.* no +ve bound.
Piperno & Depeyre	$r \in [-\infty, 0]$:0; $r \in [0,1]$:$\psi(r) = 1 + (\frac{3}{2}r + 1)(r-1)^3$; $r \in [1, +\infty]$: $\psi(r) = (3r^2 - 6r + 19)/(r^3 - 3r + 18)$ $\Psi(r) = (\frac{2}{3}r + 1/3)\psi(1/r)$	[35]	$\frac{1}{3}$	1	1	
LPPA	$r \in [-\infty, 0]$:0; $r \in [0,1]$:r$(r+3)/2(r+1)$; $r \in [1, +\infty]$:$(5r-1)/2(r+1)$	[9]	$\frac{1}{2}$	$\frac{5}{2}$	$\frac{3}{2}$	

Appendix B. Performance comparison of linear and non-linear convection schemes

Table B1 presents the results of the two scalar convection test cases discussed in Section 7.

Table B1
Performance comparison of various schemes for smooth and discontinuous test cases

Test cases		Gaussian distribution (61 × 31 grid)				Step function (81 × 41 grid)		
Scheme	Score	n	$\varepsilon \times 10^3$	N_{its}	δt_f	$\varepsilon \times 10^2$	N_{its}	δt_f
FOU	–	0.76	18.2	5	1000	167.8	12	100
κ-Schemes								
CUI ($\frac{1}{3}$)	0.84	**2.24**	0.382	29	200	6.15	51	25
Fromm's (0)	0.80	2.23	0.572	23	200	6.53	39	50
QUICK ($\frac{1}{2}$)	0.72	2.21	**0.315**	33	200	**5.92**	60	25
LUI (−1)	0.40	2.11	1.16	47	5	7.33	51	5
CDS (1)	0.24	2.07	1.12	985	30	8.99	1348	25
FL-Schemes								
MUSCL	0.78	**2.22**	0.626	59	5	5.53	107	5
OSPRE[a]	0.70	1.87	1.21	**45**	10	6.52	**61**	10
H-CUI[a]	0.69	1.88	1.03	64	10	6.07	73	5
Harmonic	0.65	1.95	1.02	61	10	6.23	107	5
SPL-$\frac{1}{3}$[a]	0.65	1.88	1.11	57	5	6.35	90	5
SMART[b]	0.62	2.11	**0.555**	143	2	**4.98**	**244**	1.5
Koren	0.62	2.08	0.635	98	2.5	5.37	121	2.5
H-QUICK[a]	0.61	1.87	1.02	75	5	5.9	77	5
SMARTER[b]	0.57	1.81	1.18	72	5	6.19	75	10
BLUI(SOU)	0.55	2.08	1.08	89	5	6.34	97	5
UMIST	0.52	1.76	1.45	58	5	6.84	65	5
GPA-$\frac{1}{2}$[a]	0.51	1.79	1.29	73	5	6.41	72	5
GPR-$\frac{1}{2}$[a]	0.51	1.77	1.34	67	5	6.47	70	5
GPR-$\frac{1}{3}$[a]	0.46	1.8	1.31	61	5	6.52	99	2.5
van Albada	0.44	1.77	1.51	63	5	7.03	68	5
Minmod	0.41	**1.58**	**2.54**	57	10	**8.45**	62	10
GVA-$\frac{1}{2}$[a]	0.33	1.74	1.49	84	5	6.76	73	5
GVA-$\frac{1}{3}$[a]	0.33	1.74	1.52	73	5	6.92	70	5
Superbee	0.28	1.23	1.62	157	2.5	**3.77**	140	10
BCDS	0.27	1.75	1.55	**483**	1	5.78	232	2

Bold: lowest or highest values
$\varepsilon = (\Sigma|\phi - \phi_{exact}|)/N_{cell}$: error in L_1 norm (sum over total number of cells, N_{cell}).
n = effective order of scheme for smooth solution, assuming: $\varepsilon \sim \Delta x^n$.
N_{its} = number of iterations to achieve convergence: (residual / net flux) < 0.05%.
δt_f = false time-step/courant time step : small $\delta t_f \Rightarrow$ strong relaxation.
Score: normalized average of rankings for n, ε and N_{its} (for both cases).
[a] Proposed in [59].
[b] Converted from NV scheme.

References

[1] R.K. Agarwal, A third-order-accurate upwind scheme for Navier–Stokes solutions at high Reynolds numbers, AIAA paper 1981-112, in: 19th AIAA Aerospace Sciences Meeting, St. Louis, MO, USA, 1981.
[2] M.A. Alves, P.J. Oliveira, F.T. Pinho, A convergent and universally bounded interpolation scheme for the treatment of advection, Int. J. Numer. Methods Fluids 41 (1) (2002) 47.
[3] M. Arora, P.L. Roe, A well-behaved TVD limiter for high-resolution calculations of unsteady flow, J. Comput. Phys. 132 (1) (1997) 3.
[4] M. Atias, M. Wolfshtein, M. Israeli, Efficiency of Navier–Stokes solvers, AIAA J. 15 (2) (1977) 263.
[5] T.J. Barth, B. Jespersen, The design and application of upwind schemes on unstructured meshes, AIAA paper 89-0366, in: 27th AIAA Aerospace Sciences Meeting, Reno, NV, USA, 1989.

[6] M. Berger, M.J. Aftosmis, S.M. Murman, Analysis of slope limiters on irregular grids, AIAA paper 2005-0490, in: 43rd AIAA Aerospace Sciences Meeting, Reno, NV, USA, 2005.
[7] M. Berzins, J.M. Ware, Positive cell-centered finite volume discretization methods for hyperbolic equations on irregular meshes, Appl. Numer. Math. 16 (1995) 417.
[8] S.R. Chakravarthy, S. Osher, High resolution applications of the Osher upwind scheme for the Euler equations, AIAA Paper 1983-1943, in: Sixth AIAA CFD Conference, Danvers, MA, USA, 1983, pp. 363.
[9] S.K. Choi, H.Y. Nam, M. Cho, A comparison of higher-order bounded convection schemes, Comput. Methods Appl. Mech. Eng. 121 (1995) 281.
[10] S.K. Choi, H.Y. Nam, M. Cho, Evaluation of a high-order bounded convection scheme: three-dimensional numerical experiments, Numer. Heat Transfer, Part B 28 (1995) 23.
[11] M.S. Darwish, A new high-resolution scheme based on the normalized variable formulation, Numer. Heat Transfer, Part B 24 (1993) 353.
[12] M.S. Darwish, F.H. Moukalled, Normalized variable and space formulation methodology for high-resolution schemes, Numer. Heat Transfer, Part B 26 (1994) 79.
[13] J.E. Fromm, A method for reducing dispersion in convective difference schemes, J. Comput. Phys. 3 (1968) 176.
[14] P.H. Gaskell, A.K.C. Lau, Curvature-compensated convective transport: SMART, a new boundedness-preserving transport algorithm, Int. J. Numer. Methods Fluids 8 (1988) 617.
[15] J.B. Goodman, R.J. Leveque, On the accuracy of stable schemes for 2D scalar conservation laws, Math. Comput. 45 (1985) 15.
[16] A. Harten, High resolution schemes for hyperbolic conservation laws, J. Comput. Phys. 49 (1983) 357.
[17] A. Holstad, The Koren upwind scheme for variable gridsize, Appl. Numer. Math. 37 (2001) 459.
[18] W. Hunsdorfer, B. Koren, M. van Loon, J.G. Verwer, A positive finite-difference advection scheme, J. Comput. Phys. 117 (1995) 35.
[19] A. Jameson, Artificial diffusion, upwind biasing, limiters and their effect on accuracy and multigrid convergence in transonic and hypersonic flows, AIAA Paper 93-3359, in: 11th AIAA CFD Conference, Orlando, FL, 1993.
[20] A. Jameson, Positive schemes and shock modelling for compressible flows, Int. J. Numer. Methods Fluids 20 (1995) 743.
[21] H. Jasak, H.G. Weller, A.D. Gosman, High resolution NVD differencing scheme for arbitrarily unstructured meshes, Int. J. Numer. Methods Fluids 31 (1999) 431.
[22] P.K. Khosla, S.G. Rubin, A diagonally dominant second order accurate implicit scheme, J. Comput. Fluids 2 (1974) 207.
[23] B. Koren, Upwind discretization of the steady Navier–Stokes equations, Int. J. Numer. Methods Fluids 11 (1) (1990) 99.
[24] B. Koren, A robust upwind discretization method for advection, diffusion and source terms, in: Vreugdenhil, Koren (Eds.), Numerical Methods for Advection–Diffusion Problems, Vieweg, Braunschweig, 1993, p. 117.
[25] B.P. Leonard, The QUICK algorithm: a uniformly third-order finite difference method for highly convective flows, Comput. Methods Appl. Mech. Eng. 19 (1979) 59.
[26] B.P. Leonard, Finite-volume methods for the compressible Navier–Stokes equations, in: Taylor, Habashi, Hafez (Eds.), Proceedings of the Fifth International Conference on Numerical Methods in Laminar and Turbulent Flow, Montreal, July, Pineridge Press, Swansea, 1987, p. 35.
[27] B.P. Leonard, Simple high-accuracy resolution program for convective modelling of discontinuities, Int. J. Numer. Methods Fluids 8 (1988) 1291.
[28] R.J. Leveque, Numerical Methods for Conservation Laws, second ed., Lectures in Mathematics, ETH Zürich, Birkhaüser, 1992.
[29] F.S. Lien, M.A. Leschziner, Upstream monotonic interpolation for scalar transport with application to complex turbulent flows, Int. J. Numer. Methods Fluids 19 (1994) 527.
[30] C.-H. Lin, C.A. Lin, Simple high-order bounded convection scheme to model discontinuities, AIAA J. 35 (3) (1997) 563.
[31] B. Noll, Evaluation of a bounded high-resolution scheme for combustor flow computations, AIAA J. 30 (1) (1992) 64.
[32] G. Papadakis, G. Bergeles, A locally-modified second-order upwind scheme for convection-term discretization, in: Taylor (Ed.), Proceedings of the Eighth International Conference on Numerical Methods in Laminar and Turbulent Flow, Swansea, July, Pineridge Press, Swansea, 1993, p. 577.
[33] A. Pascau, C. Perez, A well-behaved scheme to model strong convection in a general transport equation, in: Taylor (Ed.), Proceedings of the Eighth International Conference on Numerical Methods in Laminar and Turbulent Flow, Swansea, July, Pineridge Press, Swansea, 1993, p. 608.
[34] S.V. Patankar, Numerical Heat Transfer and Fluid Flow, Hemisphere, 1980.
[35] S. Piperno, S. Depeyre, Criteria for the design of limiters yielding efficient high resolution TVD schemes, J. Comput. Fluids 27 (1998) 183.
[36] H.S. Price, R.S. Varga, J.E. Warren, Applications of oscillation matrices to diffusion-correction equations, J. Math. Phys. 45 (1966) 301.
[37] V. Pržulj, B. Basara, Bounded convection schemes for unstructured grids, AIAA Paper 2001-2593, in: AIAA CFD Conference, Anaheim, CA, 2001.
[38] P.L. Roe, Some contributions to the modelling of discontinuous flows, in: Engquist, Osher, Somerville, (Eds.), Lectures in Applied Mathematics, Large-scale Computations in Fluid Mechanics (AMS-SIAM Summer Seminar, La Jolla, CA, USA, 1983), Am. Math. Soc., 1985, Vol. 22, Part 2, p. 163.
[39] P.L. Roe, Finite-volume methods for the compressible Navier–Stokes equations, in: Taylor, Habashi, Hafez (Eds.), Proceedings of the Fifth International Conference on Numerical Methods in Laminar and Turbulent Flow, Montreal, July, Pineridge Press, Swansea, 1987, p. 2088.
[40] P.L. Roe, Characteristic-based schemes for the Euler equations, Ann. Rev. Fluid Mech. 18 (1986) 337.

[41] P.L. Roe, M.J. Baines, Algorithms for advection and shock problems, in: Viviand (Ed.), Proceedings of the Fourth GAMM Conference on Numerical Methods in Fluid Mechanics, vol. 5, Vieweg, 1982, p. 281.
[42] B. Song, G.R. Liu, K.Y. Lam, R.S. Amano, On a higher-order bounded discretization scheme, Int. J. Numer. Methods Fluids 32 (7) (2000) 881.
[43] S.P. Spekreijse, Multigrid solution of the steady Euler equations, Doctoral Thesis, Delft University of Technology, The Netherlands, 1986.
[44] S.P. Spekreijse, Multigrid solution of monotone second-order discretizations of hyperbolic conservation laws, Report NM-R8611, Centrum voor Wiskunde en Informatica (CWI), Amsterdam, The Netherlands, 1986.
[45] D.B. Spalding, A general-purpose computer program for multi-dimensional one- and two-phase flows, IMACS Meeting, Lehigh University, Pennsylvania, 1981.
[46] P.K. Sweby, High resolution schemes using flux limiters for hyperbolic conservation laws, SIAM J. Numer. Anal. 21 (1984) 995.
[47] P.K. Sweby, High resolution TVD schemes using flux limiters, in: Engquist, Osher and Somerville (Eds.), Lectures in Applied Mathematics, Large-Scale Computations in Fluid Mechanics, (AMS-SIAM Summer Seminar, La Jolla, CA, USA, 1983), Am. Math. Soc., Vol. 22, Part 2, 1985, p. 289.
[48] G. Tiesinga, Multi-level ILU preconditioners and continuation methods in fluid dynamics, Doctoral Thesis, Rijksuniversiteit Groningen, The Netherlands, 2000.
[49] G.D. van Albada, B. van Leer, W.W. Roberts, A comparative study of computational methods in cosmic gas dynamics, Astron. Astrophys. 108 (1982) 76.
[50] B. van Leer, Towards the ultimate conservative difference scheme. II. Monotonicity and conservation combined in a second-order scheme, J. Comput. Phys. 14 (1974) 361.
[51] B. van Leer, Towards the ultimate conservative difference scheme. IV. A new approach to numerical convection, J. Comput. Phys. 23 (1977) 276.
[52] B. van Leer, Towards the ultimate conservative difference scheme. V. A second-order sequel to Godunov's method, J. Comput. Phys. 32 (1979) 101.
[53] B. van Leer, Upwind difference methods for aerodynamic problems governed by the Euler equations, in: Engquist, Osher and Somerville (Eds.), Lectures in Applied Mathematics, Large-Scale Computations in Fluid Mechanics, (AMS-SIAM Summer Seminar, La Jolla, CA, USA, 1983), Am. Math. Soc., vol. 22, Part 2, 1985, p. 327.
[54] A. Varonos, G. Bergeles, Development and assessment of a variable-order non-oscillatory scheme for convection term discretization, Int. J. Numer. Methods Fluids 26 (1) (1998) 1.
[55] V. Venkatakrishnan, Preconditioned conjugate gradient methods for the compressible Navier–Stokes equations, AIAA J. 29 (7) (1991) 1092.
[56] V. Venkatakrishnan, On the accuracy of limiters and convergence to steady state solutions, AIAA paper 93-0880, in: 31st AIAA Aerospace Sciences Meeting & Exhibit, Reno, NV, USA, 1993.
[57] R.F. Warming, R.M. Beam, Upwind second-order difference schemes and application in aerodynamics flows, AIAA J. 14 (9) (1976) 1241.
[58] N.P. Waterson, Development of a bounded higher-order convection scheme for general industrial applications, Project Report 1994-33, von Karman Institute for Fluid Dynamics, Sint-Genesius-Rode, Belgium, 1994.
[59] N.P. Waterson, H. Deconinck, A unified approach to the design and application of bounded higher-order convection schemes, in: Taylor, Durbetaki (Eds.), Proceedings of the Ninth International Conference on Numerical Methods in Laminar and Turbulent Flow, Atlanta, July, Pineridge Press, Swansea, 1995, p. 203.
[60] J.-J. Wei, B. Yu, W.-Q. Tao, Y. Kawaguchi, H.-S. Wang, A new high-order accurate and bounded scheme for incompressible flow, Numer. Heat Transfer, Part B 43 (2003) 19.
[61] B. Yu, W.-Q. Tao, D.S. Zhang, Q.W. Wang, Discussion on numerical stability and boundedness of convective discretized scheme, Numer. Heat Transfer, Part B 40 (2001) 343.
[62] G. Zhou, L. Davidson, E. Olsson, Transonic inviscid/turbulent airfoil flow simulations using a pressure-based method with high order schemes, Lecture Notes in Physics 453 (1995) 372.
[63] J. Zhu, W. Rodi, A low dispersion and bounded convection scheme, Comput. Methods Appl. Mech. Eng. 92 (1991) 87.
[64] J. Zhu, On the higher-order bounded discretization schemes for finite volume computations of incompressible flows, Comput. Methods Appl. Mech. Eng. 98 (1992) 345.
[65] M. Zijlema, On the construction of a third-order accurate monotone convection scheme with application to turbulent flows in general domains, Int. J. Numer. Methods Fluids 22 (1996).
[66] M. Zijlema, Computational modeling of turbulent flow in general domains, Doctoral Thesis, Delft University of Technology, The Netherlands, 1996.